High-dimensional covariance estimation by minimizing ℓ_1-penalized log-determinant divergence

Pradeep Ravikumar, Martin J. Wainwright,
Garvesh Raskutti and Bin Yu

Berkeley, CA 94720-1776 USA
e-mail: pradeepr@stat.berkeley.edu
wainwrig@stat.berkeley.edu
garveshr@stat.berkeley.edu
binyu@stat.berkeley.edu

Abstract: Given i.i.d. observations of a random vector $X \in \mathbb{R}^p$, we study the problem of estimating both its covariance matrix Σ^*, and its inverse covariance or concentration matrix $\Theta^* = (\Sigma^*)^{-1}$. When X is multivariate Gaussian, the non-zero structure of Θ^* is specified by the graph of an associated Gaussian Markov random field; and a popular estimator for such sparse Θ^* is the ℓ_1-regularized Gaussian MLE. This estimator is sensible even for for non-Gaussian X, since it corresponds to minimizing an ℓ_1-penalized log-determinant Bregman divergence. We analyze its performance under high-dimensional scaling, in which the number of nodes in the graph p, the number of edges s, and the maximum node degree d, are allowed to grow as a function of the sample size n. In addition to the parameters (p, s, d), our analysis identifies other key quantities that control rates: (a) the ℓ_∞-operator norm of the true covariance matrix Σ^*; and (b) the ℓ_∞ operator norm of the sub-matrix Γ^*_{SS}, where S indexes the graph edges, and $\Gamma^* = (\Theta^*)^{-1} \otimes (\Theta^*)^{-1}$; and (c) a mutual incoherence or irrepresentability measure on the matrix Γ^* and (d) the rate of decay $1/f(n, \delta)$ on the probabilities $\{|\widehat{\Sigma}^n_{ij} - \Sigma^*_{ij}| > \delta\}$, where $\widehat{\Sigma}^n$ is the sample covariance based on n samples. Our first result establishes consistency of our estimate $\widehat{\Theta}$ in the elementwise maximum-norm. This in turn allows us to derive convergence rates in Frobenius and spectral norms, with improvements upon existing results for graphs with maximum node degrees $d = o(\sqrt{s})$. In our second result, we show that with probability converging to one, the estimate $\widehat{\Theta}$ correctly specifies the zero pattern of the concentration matrix Θ^*. We illustrate our theoretical results via simulations for various graphs and problem parameters, showing good correspondences between the theoretical predictions and behavior in simulations.

AMS 2000 subject classifications: Primary 62F12; secondary 62F30.
Keywords and phrases: Covariance, concentration, precision, sparsity, Gaussian graphical models, ℓ_1 regularization.

Received January 2010.

1. Introduction

The area of high-dimensional statistics deals with estimation in the "large p, small n" setting, where p and n correspond, respectively, to the dimensional-

ity of the data and the sample size. Such high-dimensional problems arise in a variety of applications, among them remote sensing, computational biology and natural language processing, where the model dimension may be comparable or substantially larger than the sample size. It is well-known that such high-dimensional scaling can lead to dramatic breakdowns in many classical procedures. In the absence of additional model assumptions, it is frequently impossible to obtain consistent procedures when $p \gg n$. Accordingly, an active line of statistical research is based on imposing various restrictions on the model–for instance, sparsity, manifold structure, or graphical model structure–and then studying the scaling behavior of different estimators as a function of sample size n, ambient dimension p and additional parameters related to these structural assumptions.

In this paper, we study the following problem: given n i.i.d. observations $\{X^{(k)}\}_{k=1}^n$ of a zero mean random vector $X \in \mathbb{R}^p$, estimate both its covariance matrix Σ^*, and its inverse covariance or concentration matrix $\Theta^* := (\Sigma^*)^{-1}$. Perhaps the most natural candidate for estimating Σ^* is the empirical sample covariance matrix, but this is known to behave poorly in high-dimensional settings. For instance, when $p/n \to c > 0$, and the samples are drawn i.i.d. from a multivariate Gaussian distribution, neither the eigenvalues nor the eigenvectors of the sample covariance matrix are consistent estimators of the population versions [16, 17]. Accordingly, many regularized estimators have been proposed to estimate the covariance or concentration matrix under various model assumptions. One natural model assumption is that reflected in shrinkage estimators, such as in the work of Ledoit and Wolf [19], who proposed to shrink the sample covariance to the identity matrix. An alternative model assumption, relevant in particular for time series data, is that the covariance or concentration matrix is banded, meaning that the entries decay based on their distance from the diagonal. Furrer and Bengtsson [12] proposed to shrink the covariance entries based on this distance from the diagonal. Wu and Pourahmadi [30] and Huang et al. [15] estimate these banded concentration matrices by using thresholding and ℓ_1-penalties respectively, as applied to a Cholesky factor of the inverse covariance matrix. Bickel and Levina [2] prove the consistency of these banded estimators so long as $\frac{(\log p)^2}{n} \to 0$ and the model covariance matrix is banded as well, but as they note, these estimators depend on the presented order of the variables. In recent work, Cai et al. [7] have studied such banded covariance models and derived optimal rates of convergence.

A related class of models are based on positing some kind of sparsity, either in the covariance matrix, or in the inverse covariance. Bickel and Levina [1] study thresholding estimators of covariance matrices, assuming that each row satisfies an ℓ_q-ball sparsity assumption. In independent work, El Karoui [10] also studied thresholding estimators of the covariance, but based on an alternative notion of sparsity, one which captures the number of closed paths of any length in the associated graph. Other work has studied models in which the inverse covariance or concentration matrix has an elementwise sparse structure. As will be clarified in the next section, when the random vector is multivariate Gaussian,

the set of non-zero entries in the concentration matrix correspond to the set of edges in an associated Gaussian Markov random field (GMRF). In this setting, imposing sparsity on the entries of the concentration matrix can be interpreted as requiring that the graph underlying the GMRF have relatively few edges. A minimum mean-squared error estimator for such GMRFs with relatively few edges has been analyzed by Giraud [13]. Another line of recent papers [9, 11, 31] have proposed an estimator that minimizes the Gaussian negative log-likelihood regularized by the ℓ_1 norm of the entries (or the off-diagonal entries) of the concentration matrix. The resulting optimization problem is a log-determinant program, which can be solved in polynomial time with interior point methods [3], or by faster co-ordinate descent algorithms [9, 11]. In recent work, Rothman et al. [27] have analyzed some aspects of high-dimensional behavior of this estimator; assuming that the minimum and maximum eigenvalues of Σ^* are bounded, they show that consistent estimates can be achieved in Frobenius and spectral norm, in particular at the rate $\mathcal{O}(\sqrt{\frac{(s+p)\log p}{n}})$. Lam and Fan [18] analyze a generalization of this estimator based on regularizers more general than the ℓ_1 norm. For the case of ℓ_1 regularization, they too obtain the same Frobenius and spectral norm rates as the paper [27]. They also show that the ℓ_1-based estimator succeeds in recovering the zero-pattern of the concentration matrix Θ^* so long as the number of edges s scales as $s = \mathcal{O}(\sqrt{p})$, and the number of observations n scales as $n = \Omega((s+p)\log p)$.

The focus of this paper is the problem of estimating the concentration matrix Θ^* under sparsity conditions. We do not impose specific distributional assumptions on X itself, but rather analyze the estimator in terms of the tail behavior of the maximum deviation $\max_{i,j} |\widehat{\Sigma}_{ij}^n - \Sigma_{ij}^*|$ of the sample and population covariance matrices. To estimate Θ^*, we use the ℓ_1-penalized Gaussian maximum likelihood estimator that has been proposed in past work [9, 11, 31]. We show it actually corresponds to minimization of an ℓ_1-penalized log-determinant Bregman divergence and thus use it without assuming that X is necessarily multivariate Gaussian. We analyze the behavior of this estimator under high-dimensional scaling, in which the number of nodes p in the graph, and the maximum node degree d are all allowed to grow as a function of the sample size n.

In addition to the triple (n, p, d), we also explicitly keep track of certain other measures of model complexity, that could potentially scale as well. The first of these measures is the ℓ_∞-operator norm of the covariance matrix Σ^*, which we denote by $\kappa_{\Sigma^*} := |||\Sigma^*|||_\infty$. The next quantity involves the Hessian of the log-determinant objective function, $\Gamma^* := (\Theta^*)^{-1} \otimes (\Theta^*)^{-1}$. When the distribution of X is multivariate Gaussian, this Hessian has the more explicit representation $\Gamma^*_{(j,k),(\ell,m)} = \text{cov}\{X_j X_k,\ X_\ell X_m\}$, showing that it measures the covariances of the random variables associated with each edge of the graph. For this reason, the matrix Γ^* can be viewed as an edge-based counterpart to the usual node-based covariance matrix Σ^*. Using S to index the variable pairs (i, j) associated with non-zero entries in the inverse covariance. our analysis involves the quantity $\kappa_{\Gamma^*} = |||(\Gamma^*_{SS})^{-1}|||_\infty$. Finally, we also impose a mutual incoherence or irrepresentability condition on the Hessian Γ^*; this condition is similar to

assumptions imposed on Σ^* in previous work on the Lasso [22, 28, 29, 32]. We provide some examples where the Lasso irrepresentability condition holds, but our corresponding condition on Γ^* fails; however, we do not know currently whether one condition strictly dominates the other.

Our first result establishes consistency of our estimator $\widehat{\Theta}$ in the element-wise maximum-norm, providing a rate that depends on the tail behavior of the entries in the random matrix $\widehat{\Sigma}^n - \Sigma^*$. For the special case of sub-Gaussian random vectors with concentration matrices having at most d non-zeros per row (corresponding to graphs with maximal degree d) and at most s off-diagonal non-zero entries, a corollary of our analysis is consistency in spectral norm at rate $\|\widehat{\Theta} - \Theta^*\|_2 = \mathcal{O}(\sqrt{\min\{d^2 \log p, (s + p) \log p\}/n})$, with high probability. When the maximum degree d is large relative to the number of non-zeros (i.e., $d^2 \geq s$), this rate is equivalent to the spectral norm rates obtained in past work [18, 27]. However, when the graph has relatively small degrees (a special case being bounded degree), then our result provides a faster rate in spectral norm, but requires stronger conditions than the Rothman et al. [27] result. Section 3.5.2 provides a more detailed comparison between our results and this past work [18, 27]. Under the milder restriction of each element of X having bounded $4m$-th moment, we derive a rate in spectral norm that is substantially slower—namely, $\|\widehat{\Theta} - \Theta^*\|_2 = \mathcal{O}(d \, p^{1/2m}/\sqrt{n})$—showing that the familiar logarithmic dependence on the model size p is linked to particular tail behavior of the distribution of X. Finally, we show that under the same scalings as above, with probability converging to one, the estimate $\widehat{\Theta}$ correctly specifies the zero pattern of the concentration matrix Θ^*.

The remainder of this paper is organized as follows. In Section 2, we set up the problem and give some background. Section 3 is devoted to statements of our main results, as well as discussion of their consequences. Section 4 provides an outline of the proofs, with the more technical details deferred to appendices. In Section 5, we report the results of some simulation studies that illustrate our theoretical predictions.

Notation For the convenience of the reader, we summarize here notation to be used throughout the paper. Given a vector $u \in \mathbb{R}^d$ and parameter $a \in [1, \infty]$, we use $\|u\|_a$ to denote the usual ℓ_a norm. Given a matrix $U \in \mathbb{R}^{p \times p}$ and parameters $a, b \in [1, \infty]$, we use $\|U\|_{a,b}$ to denote the induced matrix-operator norm $\max_{\|y\|_a=1} \|Uy\|_b$; see Horn and Johnson [14] for background. Three cases of particular importance in this paper are the *operator norm* $\|U\|_2$, which is equal to the maximal singular value of U; the ℓ_∞/ℓ_∞-*operator norm*, given by

$$\|U\|_\infty \quad := \quad \max_{j=1,\ldots,p} \sum_{k=1}^{p} |U_{jk}|, \tag{1}$$

and the ℓ_1/ℓ_1-*operator norm*, given by $\|U\|_1 = \|U^T\|_\infty$. Finally, we use $\|U\|_\infty$ to denote the element-wise maximum $\max_{i,j} |U_{ij}|$; note that this is not a matrix norm, but rather a norm on the vectorized form of the matrix. For any matrix $U \in \mathbb{R}^{p \times p}$, we use $\text{vec}(U)$ or equivalently $\overline{U} \in \mathbb{R}^{p^2}$ to denote its *vectorized*

form, obtained by stacking up the rows of U. We use $\langle\!\langle U,\, V \rangle\!\rangle := \sum_{i,j} U_{ij} V_{ij}$ to denote the *trace inner product* on the space of symmetric matrices. Note that this inner product induces the *Frobenius norm* $\|U\|_F := \sqrt{\sum_{i,j} U_{ij}^2}$. Finally, for asymptotics, we use the following standard notation: we write $f(n) = \mathcal{O}(g(n))$ if $f(n) \le c g(n)$ for some constant $c < \infty$, and $f(n) = \Omega(g(n))$ if $f(n) \ge c' g(n)$ for some constant $c' > 0$. The notation $f(n) \asymp g(n)$ means that $f(n) = \mathcal{O}(g(n))$ and $f(n) = \Omega(g(n))$. Furthermore, we recall the standard matrix notation $\succ$ and $\succeq$. For two $k \times k$ matrices A and B, $A \succ B$ means that $A - B$ is positive definite and $A \succeq B$ mean $A - B$ is positive semi-definite. For a matrix C and a set of tuples S, C_S denotes the set of numbers $(C_{(j,k)})_{(j,k)\in S}$.

2. Background and problem set-up

Let $X = (X_1, \ldots, X_p)$ be a zero mean p-dimensional random vector. The focus of this paper is the problem of estimating the covariance matrix $\Sigma^* := \mathbb{E}[XX^T]$ and concentration matrix $\Theta^* := \Sigma^{*-1}$ of the random vector X given n i.i.d. observations $\{X^{(k)}\}_{k=1}^n$. In this section, we provide background, and set up this problem more precisely. We begin by describing Gaussian graphical models, which provide motivation for estimation of (sparse) concentration matrices. We then describe an estimator based on minimizing an ℓ_1-regularized log-determinant divergence; when the data are drawn from a Gaussian graphical model, this estimator corresponds to ℓ_1-regularized maximum likelihood. We conclude by discussing various distributional assumptions that we consider in this paper.

2.1. Gaussian graphical models

One motivation for this paper is the problem of Gaussian graphical model selection. Let $X = (X_1, X_2, \ldots, X_p)$ denote a zero-mean Gaussian random vector; its density can be parameterized by the inverse covariance or *concentration matrix* $\Theta^* = (\Sigma^*)^{-1} \succ 0$, and can be written as

$$f(x_1, \ldots, x_p; \Theta^*) \;\; = \;\; \frac{1}{\sqrt{(2\pi)^p \det((\Theta^*)^{-1})}} \; \exp\left\{ -\frac{1}{2} x^T \Theta^* x \right\}. \qquad (2)$$

Suppose that the variables $(X_1, \ldots, X_p)$ are associated with the vertex set $V = \{1, 2, \ldots, p\}$ of an undirected graph $G = (V, E)$. We say that the concentration matrix Θ^* respects the edge structure[1] of the graph if $\Theta_{ij}^* = 0$ for all $(i, j) \notin E$. The family of Gaussian distributions with this property is known as a Gauss-Markov random field with respect to the graph G. Figure 1 illustrates this correspondence between the graph structure (panel (a)), and the sparsity pattern of the concentration matrix Θ^* (panel (b)). The problem of estimating the entries of the concentration matrix Θ^* corresponds to parameter

---

[1] As a remark on notation, note the difference between this edge set E and the expectation $\mathbb{E}$ of a random variable.
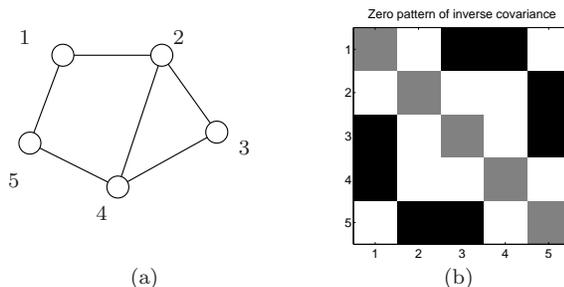
FIG 1. *(a) Simple undirected graph. A Gauss Markov random field has a Gaussian variable X_i associated with each vertex $i \in V$. This graph has $p = 5$ vertices, maximum degree $d = 3$ and $s = 6$ edges. (b) Zero pattern of the inverse covariance Θ^* associated with the GMRF in (a). The set $E(\Theta^*)$ corresponds to the off-diagonal non-zeros (white blocks); the diagonal is also non-zero (grey squares), but these entries do not correspond to edges. The black squares correspond to non-edges, or zeros in Θ^*.*

estimation, while the problem of determining which off-diagonal entries of Θ^* are non-zero—that is, the set

$$E(\Theta^*) \quad := \quad \{i, j \in V \mid i \neq j, \Theta_{ij}^* \neq 0\}, \tag{3}$$

corresponds to the problem of Gaussian graphical *model selection.*

With a slight abuse of notation, we define the *sparsity index* $s := |E(\Theta^*)|$ as the total number of non-zero elements in off-diagonal positions of Θ^*; equivalently, this corresponds to twice the number of edges in the case of a Gaussian graphical model. We also define the *maximum degree or row cardinality*

$$d \quad := \quad \max_{i=1,\ldots,p} \left| \left\{ j \in V \mid \Theta_{ij}^* \neq 0 \right\} \right|, \tag{4}$$

corresponding to the maximum number of non-zeros in any row of Θ^*; this corresponds to the maximum degree in the graph of the underlying Gaussian graphical model. Note that we have included the diagonal entry Θ_{ii}^* in the degree count, corresponding to a self-loop at each vertex.

It is convenient throughout the paper to use graphical terminology, such as degrees and edges, even though the distributional assumptions that we impose, as described in Section 2.3, are milder and hence apply even to distributions that are not Gaussian MRFs.

2.2. ℓ_1-penalized log-determinant divergence

An important set in this paper is the cone

$$\mathcal{S}_+^p \quad := \quad \left\{ A \in \mathbb{R}^{p \times p} \mid A = A^T,\ A \succeq 0 \right\}, \tag{5}$$

formed by all symmetric positive semi-definite matrices in p dimensions. We assume that the covariance matrix Σ^* and concentration matrix Θ^* of

the random vector X are strictly positive definite, and so lie in the interior $\mathcal{S}_{++}^p := \left\{ A \in \mathbb{R}^{p \times p} \mid A = A^T, \ A \succ 0 \right\}$ of the cone $\mathcal{S}_+^p$.

The focus of this paper is a particular type of M-estimator for the concentration matrix Θ^*, based on minimizing a Bregman divergence between positive definite matrices. A function is of Bregman type if it is strictly convex, continuously differentiable and has bounded level sets [4, 8]. Any such function induces a *Bregman divergence* of the form $D_g(A\|B) = g(A) - g(B) - \langle \nabla g(B), A - B \rangle$. From the strict convexity of g, it follows that $D_g(A\|B) \geq 0$ for all A and B, with equality if and only if $A = B$.

As a candidate Bregman function, consider the log-determinant barrier function, defined for any matrix $A \in \mathcal{S}_+^p$ by

$$g(A) \quad := \quad \begin{cases} -\log\det(A) & \text{if } A \succ 0 \\ +\infty & \text{otherwise.} \end{cases} \tag{6}$$

As is standard in convex analysis, we view this function as taking values in the extended reals $\mathbb{R}_* = \mathbb{R} \cup \{+\infty\}$. With this definition, the function g is strictly convex, and its domain is the set of strictly positive definite matrices. Moreover, it is continuously differentiable over its domain, with $\nabla g(A) = -A^{-1}$; see Boyd and Vandenberghe [3] for further discussion. The Bregman divergence corresponding to this log-determinant Bregman function g is given by

$$D_g(A\|B) \quad := \quad -\log\det A + \log\det B + \langle\!\langle B^{-1}, \ A - B \rangle\!\rangle, \tag{7}$$

valid for any $A, B \in \mathcal{S}_+^p$ that are strictly positive definite. This divergence suggests a natural way to estimate concentration matrices—namely, by minimizing the divergence $D_g(\Theta\|\Theta^*)$—or equivalently, by minimizing the function

$$\min_{\Theta \succ 0} \left\{ \langle\!\langle \Theta, \ \Sigma^* \rangle\!\rangle - \log\det\Theta \right\}, \tag{8}$$

where we have discarded terms independent of Θ, and used the fact that the inverse of the concentration matrix is the covariance matrix (i.e., $(\Theta^*)^{-1} = \Sigma^* = \mathbb{E}[XX^T]$). Of course, the convex program (8) cannot be solved without knowledge of the true covariance matrix Σ^*, but one can take the standard approach of replacing Σ^* with an empirical version, with the possible addition of a regularization term.

In this paper, we analyze a particular instantiation of this strategy. Given n samples, we define the *sample covariance matrix*

$$\widehat{\Sigma}^n \quad := \quad \frac{1}{n} \sum_{k=1}^n X^{(k)}(X^{(k)})^T. \tag{9}$$

To lighten notation, we occasionally drop the superscript n, and simply write $\widehat{\Sigma}$ for the sample covariance. We also define the *off-diagonal ℓ_1 regularizer*

$$\|\Theta\|_{1,\text{off}} \quad := \quad \sum_{i \neq j} |\Theta_{ij}|, \tag{10}$$

where the sum ranges over all $i, j = 1, \ldots, p$ with $i \neq j$. Given some regularization constant $\lambda_n > 0$, we consider estimating Θ^* by solving the following ℓ_1-*regularized log-determinant program*:

$$\widehat{\Theta} \ := \ \arg \min_{\Theta \in \mathcal{S}_{++}^p} \left\{ \langle\!\langle \Theta, \, \widehat{\Sigma}^n \rangle\!\rangle - \log \det(\Theta) + \lambda_n \|\Theta\|_{1,\text{off}} \right\}, \tag{11}$$

which returns a symmetric positive definite matrix $\widehat{\Theta}$. As shown in Appendix A, for any $\lambda_n > 0$ and sample covariance matrix $\widehat{\Sigma}^n$ with strictly positive diagonal entries, this convex optimization problem has a unique optimum, so there is no ambiguity in equation (11). When the data is actually drawn from a multivariate Gaussian distribution, then the problem (11) is simply ℓ_1-regularized maximum likelihood. As described in Section 2.1, the equality $\Theta_{ij} = 0$ indicates the absence of an edge between nodes i and j for the corresponding Gaussian graphical model, so the penalty $\|\Theta\|_{1,\text{off}}$ encourages a sparse graphical model.

Remarks   It is worth noting that in principle, one could use other Bregman divergences D_g in the population equation (8); examples include the von Neumann Entropy $D_{vn}(A\|B) = \text{Tr}[A(\log A - \log B) - A + B]$, or the Frobenius divergence, $D_F(A\|B) = \|\text{vec}(A) - \text{vec}(B)\|_2^2$. These different choices would lead to alternative forms of regularized divergence minimizations (11) for estimating the concentration matrix, and are an interesting direction for future work. Let us remark here on three properties of the log-determinant Bregman function (6) that make it especially suitable to estimating the concentration matrix. First, the log-determinant function acts as a barrier to the positive definite cone $\mathcal{S}_+$ (see Boyd and Vandenberghe [3]). This makes the corresponding problem (11) easier to optimize, and has been taken advantage of by the optimization algorithms in [9, 11]. Second, it is also helpful that the population optimization problem (8) involves only the population covariance Σ^* and not its inverse Θ^*; this feature allowed us to take the standard approach of replacing Σ^* with an empirical version $\widehat{\Sigma}$ (and adding the regularization function). In contrast, substituting other divergences $D_g(\Theta\|\Theta^*)$ for instance the Frobenius divergence in (8) could involve the population concentration matrix Θ^* itself, for which no ready sample version exists in high-dimensional regimes (since the sample covariance matrix $\widehat{\Sigma}$ is not invertible if $p > n$.) Third, the log-determinant divergence gives rise to likelihood in the multivariate Gaussian case.

We also observe that the diagonal entries of the covariance matrix Σ^* correspond to variances, while its off-diagonal entries correspond to pairwise covariances. For a general random vector, the diagonal and off-diagonal entries of the concentration matrix Θ^* do not lend themselves to natural interpretations. However, when X is multivariate Gaussian, as discussed in Section 2.1, the off-diagonal entries of Θ^* correspond to the edge-weights in the corresponding Gaussian graphical model. Consequently, imposing a prior preference for sparse graphs is a natural motivation for using the regularizer (10), corresponding to the ℓ_1-norm applied to the off-diagonal entries of the concentration matrix. Of course, other priors, on either the covariance or concentration matrix, could well motivate the use of different regularization functions.

2.3. Tail conditions

In this section, we describe the tail conditions that underlie our analysis. Since the estimator (11) is based on using the sample covariance $\widehat{\Sigma}^n$ as a surrogate for the (unknown) covariance Σ^*, any type of consistency requires bounds on the difference $\widehat{\Sigma}^n - \Sigma^*$. In particular, we define the following tail condition:

Definition 1 (Tail conditions). The random vector X satisfies tail condition $\mathcal{T}(f, v_*)$ if there exists a constant $v_* \in (0, \infty]$ and a function $f : \mathbb{N} \times (0, \infty) \to (0, \infty)$ such that for any $(i, j) \in V \times V$:

$$\mathbb{P}[|\widehat{\Sigma}^n_{ij} - \Sigma^*_{ij}| \geq \delta] \quad \leq \quad 1/f(n, \delta) \qquad \text{for all } \delta \in (0, 1/v_*]. \tag{12}$$

We adopt the convention $1/0 := +\infty$, so that the value $v_* = 0$ indicates the inequality holds for any $\delta \in (0, \infty)$.

Two important examples of the tail function f are the following:

(a) an *exponential-type tail function*, meaning that $f(n, \delta) = \exp(c\, n\, \delta^a)$, for some scalar $c > 0$, and exponent $a > 0$; and

(b) a *polynomial-type tail function*, meaning that $f(n, \delta) = c\, n^m\, \delta^{2m}$, for some positive integer $m \in \mathbb{N}$ and scalar $c > 0$.

As might be expected, if X is multivariate Gaussian, then the deviations of sample covariance matrix have an exponential-type tail function with $a = 2$. A bit more generally, in the following subsections, we provide broader classes of distributions whose sample covariance entries satisfy exponential and a polynomial tail bounds (see Lemmata 1 and 2 respectively).

Given a larger number of samples n, we expect the tail probability bound $1/f(n, \delta)$ to be smaller, or equivalently, for the tail function $f(n, \delta)$ to larger. Accordingly, we require that f is monotonically increasing in n, so that for each fixed $\delta > 0$, we can define the inverse function

$$\bar{n}_f(\delta; r) \quad := \quad \arg\max \{n \mid f(n, \delta) \leq r\}. \tag{13}$$

Similarly, we expect that f is monotonically increasing in δ, so that for each fixed n, we can define the inverse in the second argument

$$\bar{\delta}_f(r; n) \quad := \quad \arg\max \{\delta \mid f(n, \delta) \leq r\}, \tag{14}$$

where $r \in [1, \infty)$. For future reference, we note a simple consequence of the monotonicity of the tail function f—namely

$$n > \bar{n}_f(\delta, r) \quad \text{for some } \delta > 0 \quad \implies \quad \bar{\delta}_f(n, r) \leq \delta. \tag{15}$$

The inverse functions $\bar{n}_f$ and $\bar{\delta}_f$ play an important role in describing the behavior of our estimator. We provide concrete examples in the following two subsections.

2.3.1. Sub-Gaussian distributions

In this subsection, we study the case of i.i.d. observations of sub-Gaussian random variables.

Definition 2. A zero-mean random variable Z is *sub-Gaussian* if there exists a constant $\sigma \in (0, \infty)$ such that

$$\mathbb{E}[\exp(tZ)] \leq \exp(\sigma^2 t^2 / 2) \qquad \text{for all } t \in \mathbb{R}. \tag{16}$$

By the Chernoff bound, this upper bound (16) on the moment-generating function implies a two-sided tail bound of the form

$$\mathbb{P}[|Z| > z] \leq 2 \exp\left(-\frac{z^2}{2\sigma^2}\right). \tag{17}$$

Naturally, any zero-mean Gaussian variable with variance σ^2 satisfies the bounds (16) and (17). In addition to the Gaussian case, the class of sub-Gaussian variates includes any bounded random variable (e.g., Bernoulli, multinomial, uniform), any random variable with strictly log-concave density [6, 20], and any finite mixture of sub-Gaussian variables.

The following lemma, proved in Appendix D, shows that the entries of the sample covariance based on i.i.d. samples of sub-Gaussian random vector satisfy an exponential-type tail bound with exponent $a = 2$. The argument is along the lines of a result due to Bickel and Levina [1], but with more explicit control of the constants in the error exponent:

Lemma 1. *Consider a zero-mean random vector* $(X_1, \ldots, X_p)$ *with covariance* Σ^* *such that each* $X_i / \sqrt{\Sigma_{ii}^*}$ *is sub-Gaussian with parameter* σ*. Given* n *i.i.d. samples, the associated sample covariance* $\widehat{\Sigma}^n$ *satisfies the tail bound*

$$\mathbb{P}\big[|\widehat{\Sigma}_{ij}^n - \Sigma_{ij}^*| > \delta\big] \leq 4 \exp\left\{ -\frac{n\delta^2}{128(1 + 4\sigma^2)^2 \max_i(\Sigma_{ii}^*)^2} \right\},$$

for all $\delta \in \big(0, \max_i(\Sigma_{ii}^*)\, 8(1 + 4\sigma^2)\big)$*.*

Thus, the sample covariance entries the tail condition $\mathcal{T}(f, v_*)$ with $v_* = \big[\max_i(\Sigma_{ii}^*)\, 8(1 + 4\sigma^2)\big]^{-1}$, and an exponential-type tail function with $a = 2$—namely

$$f(n, \delta) = \frac{1}{4} \exp(c_* n \delta^2), \quad \text{with} \quad c_* = \big[128(1 + 4\sigma^2)^2 \max_i(\Sigma_{ii}^*)^2\big]^{-1} (18)$$

A little calculation shows that the associated inverse functions take the form

$$\bar{\delta}_f(r; n) = \sqrt{\frac{\log(4\, r)}{c_*\, n}}, \quad \text{and} \quad \bar{n}_f(r; \delta) = \frac{\log(4\, r)}{c_*\, \delta^2}. \tag{19}$$

2.3.2. Tail bounds with moment bounds

In the following lemma, proved in Appendix E, we show that given i.i.d. observations from random variables with bounded moments, the sample covariance entries satisfy a polynomial-type tail bound. See the book by Petrov [24] for related results on tail bounds for variables with bounded moments.

Lemma 2. *Suppose there exists a positive integer m and scalar $K_m \in \mathbb{R}$ such that for $i = 1, \ldots, p$,*

$$\mathbb{E}\left[\left(\frac{X_i}{\sqrt{\Sigma_{ii}^*}}\right)^{4m}\right] \leq K_m. \tag{20}$$

For i.i.d. samples $\{X_i^{(k)}\}_{k=1}^n$, the sample covariance matrix $\widehat{\Sigma}^n$ satisfies the bound

$$\mathbb{P}\left[\left|\widehat{\Sigma}_{ij}^n - \Sigma_{ij}^*\right| > \delta\right] \leq \frac{\left\{2^{2m}(\max_i \Sigma_{ii}^*)^{2m} C_m(K_m + 1)\right\}}{n^m \, \delta^{2m}}, \tag{21}$$

where C_m is a constant depending only on m.

Thus, in this case, the sample covariance satisfies the tail condition $\mathcal{T}(f, v_*)$ with $v_* = 0$, so that the bound holds for all $\delta \in (0, \infty)$, and with the polynomial-type tail function

$$f(n, \delta) = c_* n^m \delta^{2m} \quad \text{where } c_* = 1/\left\{2^{2m}(\max_i \Sigma_{ii}^*)^{2m}(K_m + 1)\right\}. \tag{22}$$

Finally, a little calculation shows that in this case, the inverse tail functions take the form

$$\bar{\delta}_f(n, r) = \frac{(r/c_*)^{1/2m}}{\sqrt{n}}, \quad \text{and} \quad \bar{n}_f(\delta, r) = \frac{(r/c_*)^{1/m}}{\delta^2}. \tag{23}$$

3. Main results and some consequences

In this section, we state our main results, and discuss some of their consequences. We begin in Section 3.1 by stating some conditions on the true concentration matrix Θ^* required in our analysis, including a particular type of incoherence or irrepresentability condition. Section 3.1.2 is devoted to illustrations of our irrepresentability assumption for some simple graphs. In Section 3.2, we state our first main result—namely, Theorem 1 on consistency of the estimator $\widehat{\Theta}$, and the rate of decay of its error in elementwise ℓ_∞ norm. Section 3.3 is devoted to Theorem 2 on the model selection consistency of the estimator. In Section 3.4, we state and prove some corollaries of Theorem 1, regarding rates in Frobenius and spectral norms. Finally, in Section 3.5 we compare our results to some related works, including a discussion on the relation between the log-determinant estimator and the ordinary Lasso (neighborhood-based approach) as methods for graphical model selection.

3.1. *Conditions on covariance and Hessian*

Our results involve some quantities involving the Hessian of the log-determinant barrier (6), evaluated at the true concentration matrix Θ^*. Using standard results on matrix derivatives [3], it can be shown that this Hessian takes the form

$$\Gamma^* \quad := \quad \nabla^2_\Theta g(\Theta)\Big|_{\Theta=\Theta^*} \quad = \quad \Theta^{*-1} \otimes \Theta^{*-1}, \tag{24}$$

where $\otimes$ denotes the Kronecker matrix product. By definition, Γ^* is a $p^2 \times p^2$ matrix indexed by vertex pairs, so that entry $\Gamma^*_{(j,k),(\ell,m)}$ corresponds to the second partial derivative $\frac{\partial^2 g}{\partial\Theta_{jk}\partial\Theta_{\ell m}}$, evaluated at $\Theta = \Theta^*$. When X has multivariate Gaussian distribution, then Γ^* is the Fisher information of the model, and by standard results on cumulant functions in exponential families [5], we have the more specific expression $\Gamma^*_{(j,k),(\ell,m)} = \mathrm{cov}\{X_j X_k,\ X_\ell X_m\}$. For this reason, Γ^* can be viewed as an edge-based counterpart to the usual covariance matrix Σ^*.

The set of non-zero off-diagonal entries in the model concentration matrix is denoted

$$E(\Theta^*) \quad := \quad \{(i,j) \in V \times V \mid i \neq j, \Theta^*_{ij} \neq 0\}, \tag{25}$$

and we let $S(\Theta^*) = \{E(\Theta^*) \cup \{(1,1),\ldots,(p,p)\}$ be the augmented set including the diagonal elements. We use $S^c(\Theta^*)$ to denote the complement of $S(\Theta^*)$ in the set $\{1,\ldots,p\} \times \{1,\ldots,p\}$, corresponding to all pairs (ℓ,m) for which $\Theta^*_{\ell m} = 0$. When it is clear from context, we adopt the shorthand S and S^c respectively; also note that $|S| = |E(\Theta^*)| + p = s + p$. Finally, for any two subsets T and T' of $V \times V$, we use $\Gamma^*_{TT'}$ to denote the $|T| \times |T'|$ matrix with rows and columns of Γ^* indexed by T and T' respectively.

Our main results involve the ℓ_∞/ℓ_∞ norm applied to the covariance matrix Σ^*, and to the inverse of a sub-block of the Hessian Γ^*. First, we define the term

$$\kappa_{\Sigma^*} \quad := \quad |\!|\!|\Sigma^*|\!|\!|_\infty \quad = \quad \left(\max_{i=1,\ldots,p}\sum_{j=1}^{p}|\Sigma^*_{ij}|\right), \tag{26}$$

corresponding to the ℓ_∞-operator norm of the true covariance matrix Σ^*. Now consider the the matrix

$$\Gamma^*_{SS} := [\Theta^{*-1} \otimes \Theta^{*-1}]_{SS} \in \mathbb{R}^{(s+p)\times(s+p)},$$

and the parameter

$$\kappa_{\Gamma^*} \quad := \quad |\!|\!|(\Gamma^*_{SS})^{-1}|\!|\!|_\infty. \tag{27}$$

Our analysis keeps explicit track of these quantities, so that they can scale in a non-trivial manner with the problem dimension p.

Finally, we assume the Hessian satisfies the following type of *mutual incoherence or irrepresentability condition*:

Assumption 1. There exists some $\alpha \in (0, 1]$ such that

$$\max_{e \in S^c} \|\Gamma_{eS}^*(\Gamma_{SS}^*)^{-1}\|_1 \leq (1 - \alpha). \tag{28}$$

The underlying intuition is that this assumption limits the influence that the non-edge terms, indexed by S^c, can have on the edge-based terms, indexed by S. To elaborate on this intuition, let us define the zero-mean *edge random variables* by

$$Y_{(j,k)} := X_j X_k - \mathbb{E}[X_j X_k], \qquad \text{for all } j, k \in \{1, 2, \ldots, p\},$$

and note that $\Gamma_{(j,k),(\ell,m)}^* = \mathbb{E}[Y_{(j,k)} Y_{(\ell,m)}]$. Defining the vector $Y_S := \{Y_{(j,k)}, (j, k) \in S\}$, then the incoherence condition reduces to

$$\max_{e \in S^c} \|\mathbb{E}(Y_e Y_S^T)\,\mathbb{E}(Y_S Y_S^T)^{-1}\|_1 \leq (1 - \alpha).$$

This condition shares an exact parallel with the incoherence condition for the Lasso [22, 28, 32], except as applied to the edge variables $Y_{(j,k)}$ as opposed to the node variables X_j. It enforces the requirement that there should be no edge variable $Y_{(j,k)}$ that is *not* included in the graph (i.e., $(j, k) \in S^c$) that is highly correlated with variables within the true edge-set E_S. In the following section, we illustrate the form taken by Assumption 1 for some concrete cases of graphical models.

A remark on notation: although our analysis allows the quantities $\kappa_{\Sigma^*}, \kappa_{\Gamma^*}$ as well as the model size p and maximum node-degree d to grow with the sample size n, we suppress this dependence on n so as to simplify notation.

3.1.1. Illustration of irrepresentability: Diamond graph

Consider the following Gaussian graphical model example from Meinshausen [21]. Figure 2(a) shows a diamond-shaped graph $G = (V, E)$, with vertex set $V = \{1, 2, 3, 4\}$ and with all edges *except* $(1, 4)$. Introducing a parameter $\rho \in$
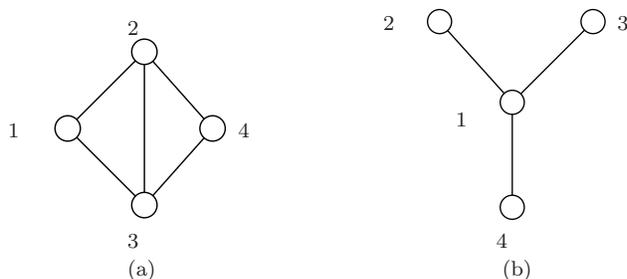

FIG 2. *(a) Graph of the example discussed by Meinshausen [21]. (b) A simple 4-node star graph.*

$[0, 1/\sqrt{2}]$, we consider the family of covariance matrices Σ^* with diagonal entries $\Sigma^*_{ii} = 1$ for all $i \in V$; off-diagonal elements $\Sigma^*_{ij} = \rho$ for all edges $(i, j) \in E \backslash \{(2, 3)\}$; $\Sigma^*_{23} = 0$; and finally the entry corresponding to the non-edge $(1, 4)$ is set as $\Sigma^*_{14} = 2\rho^2$. It can verified that $(\Sigma^*)^{-1}$ respects the structure of the graph. For this family, Meinshausen [21] showed that—for any sample size—the ℓ_1-penalized log-determinant estimator $\widehat{\Theta}$ fails to recover the graph structure if $\rho > -1 + (3/2)^{1/2} \approx 0.23$. It is instructive to compare this necessary condition to the sufficient condition provided in our analysis, namely the incoherence Assumption 1 as applied to the Hessian Γ^*. For this particular example, a little calculation shows that Assumption 1 is equivalent to the constraint

$$4|\rho|(|\rho| + 1) \quad < \quad 1,$$

an inequality which holds for all $\rho \in (-0.2017, 0.2017)$. Note that the upper value 0.2017 is just below the necessary threshold discussed by Meinshausen [21]. We can also compare this to the irrepresentability conditions for the Lasso problems obtained by regressing each node on its neighbors (see the discussion of the neighborhood-based approach of Meinshausen and Bühlmann [22] in Section 3.5.1); which requires only that $2|\rho| < 1$, i.e., $\rho \in (-0.5, 0.5)$. Thus, in the regime $|\rho| \in [0.2017, 0.5)$, the irrepresentability condition for the neighborhood-based approach holds while the log-determinant counterpart fails.

3.1.2. Illustration of irrepresentability: Star graphs

A second interesting example is the star-shaped graphical model, illustrated in Figure 2(b), which consists of a single hub node connected to the rest of the spoke nodes. We consider a four node graph, with vertex set $V = \{1, 2, 3, 4\}$ and edge-set $E = \{(1, a) \mid a \in \{2, 3, 4\}\}$. The covariance matrix Σ^* is parameterized by the correlation parameter $\rho \in [-1, 1]$: the diagonal entries are set to $\Sigma^*_{ii} = 1$, for all $i \in V$; the entries corresponding to edges are set to $\Sigma^*_{ij} = \rho$ for $(i, j) \in E$; while the non-edge entries are set as $\Sigma^*_{ij} = \rho^2$ for $(i, j) \notin E$. Consequently, for this particular example, Assumption 1 reduces to the constraint $|\rho|(|\rho| + 2) < 1$, which holds for all $\rho \in (-0.414, 0.414)$. On the other hand, the irrepresentability condition for the nodewise Lasso problems (cf. the neighborhood-based approach in Meinshausen and Bühlmann [22]) allows for the full range $\rho \in (-1, 1)$. Thus, there is again an interval $|\rho| \in [0.414, 1)$ in which the irrepresentability condition for the neighborhood-based approach holds while the log-determinant counterpart fails.

3.2. Rates in elementwise ℓ_∞-norm

We begin with a result that provides sufficient conditions on the sample size n for bounds in the elementwise ℓ_∞-norm. This result is stated in terms of the tail function f, and its inverses $\bar{n}_f$ and $\bar{\delta}_f$ (equations (13) and (14)), and so covers a general range of possible tail behaviors. So as to make it more concrete, we

follow the general statement with corollaries for the special cases of exponential-type and polynomial-type tail functions, corresponding to sub-Gaussian and moment-bounded variables respectively.

In the theorem statement, the choice of regularization constant λ_n is specified in terms of a user-defined parameter $\tau > 2$. Larger choices of τ yield faster rates of convergence in the probability with which the claims hold, but also lead to more stringent requirements on the sample size.

Theorem 1. *Consider a distribution satisfying the incoherence assumption* (28) *with parameter $\alpha \in (0, 1]$, and the tail condition* (12) *with parameters $\mathcal{T}(f, v_*)$. Let $\widehat{\Theta}$ be the unique solution (cf. Lemma 3 on page 957) of the log-determinant program* (11) *with regularization parameter $\lambda_n = (8/\alpha)\, \bar{\delta}_f(n, p^\tau)$ for some $\tau > 2$. Then, if the sample size is lower bounded as*

$$n \;>\; \bar{n}_f\left(1\Big/\max\left\{v_*,\; 6\big(1+8\alpha^{-1}\big)\,d\,\max\{\kappa_{\Sigma^*}\kappa_{\Gamma^*}, \kappa_{\Sigma^*}^3\kappa_{\Gamma^*}^2\}\right\},\; p^\tau\right), \quad (29)$$

then with probability greater than $1 - 1/p^{\tau-2} \to 1$, we have:

(a) *The estimate $\widehat{\Theta}$ satisfies the elementwise ℓ_∞-bound:*

$$\|\widehat{\Theta} - \Theta^*\|_\infty \;\leq\; \left\{2\big(1+8\alpha^{-1}\big)\kappa_{\Gamma^*}\right\}\bar{\delta}_f(n, p^\tau). \quad (30)$$

(b) *It specifies an edge set $E(\widehat{\Theta})$ that is a subset of the true edge set $E(\Theta^*)$, and includes all edges (i, j) with $|\Theta_{ij}^*| > \left\{2(1+8\alpha^{-1})\kappa_{\Gamma^*}\right\}\bar{\delta}_f(n, p^\tau)$.*

If we assume that the various quantities $\kappa_{\Gamma^*}, \kappa_{\Sigma^*}, \alpha$ remain constant as a function of (n, p, d), we have the elementwise ℓ_∞ bound $\|\widehat{\Theta} - \Theta^*\|_\infty = \mathcal{O}(\bar{\delta}_f(n, p^\tau))$, so that the inverse tail function $\bar{\delta}_f(n, p^\tau)$ from equation (14) specifies rate of convergence in the element-wise ℓ_∞-norm. In the following section, we derive the consequences of this ℓ_∞-bound for two specific tail functions, namely those of exponential-type with $a = 2$, and polynomial-type tails (see Section 2.3). Turning to the other factors involved in the theorem statement, the quantities κ_{Σ^*} and κ_{Γ^*} measure the sizes of the entries in the covariance matrix Σ^* and inverse Hessian $(\Gamma^*)^{-1}$ respectively. Finally, the factor $(1 + \frac{8}{\alpha})$ depends on the irrepresentability condition, growing in particular as the incoherence parameter α approaches 0.

3.2.1. Exponential-type tails

We now discuss the consequences of Theorem 1 for distributions in which the sample covariance satisfies an exponential-type tail bound with exponent $a = 2$. In particular, recall from Lemma 1 that such a tail bound holds when the variables are sub-Gaussian.

Corollary 1. *Under the same conditions as Theorem 1, suppose moreover that the variables $X_i/\sqrt{\Sigma_{ii}^*}$ are sub-Gaussian with parameter σ, and the samples are*

drawn independently. Then if the sample size n satisfies the bound

$$n \quad > \quad C_1 \, d^2 \left(1 + \frac{8}{\alpha}\right)^2 \left(\tau \log p + \log 4\right) \tag{31}$$

where $C_1 := \left\{48\sqrt{2}\,(1 + 4\sigma^2)\, \max_i(\Sigma_{ii}^*)\, \max\{\kappa_{\Sigma^*}\kappa_{\Gamma^*}, \kappa_{\Sigma^*}^3\kappa_{\Gamma^*}^2\}\right\}^2$, then with probability greater than $1 - 1/p^{\tau-2}$, the estimate $\widehat{\Theta}$ satisfies the bound,

$$\|\widehat{\Theta} - \Theta^*\|_\infty \quad \leq \quad \left\{16\sqrt{2}\,(1 + 4\sigma^2)\, \max_i(\Sigma_{ii}^*)\,(1 + 8\alpha^{-1})\kappa_{\Gamma^*}\right\} \sqrt{\frac{\tau \log p + \log 4}{n}}.$$

Proof. From Lemma 1, when the rescaled variables $X_i/\sqrt{\Sigma_{ii}^*}$ are sub-Gaussian with parameter σ, the sample covariance entries satisfies a tail bound $\mathcal{T}(f, v_*)$ with with $v_* = \left[\max_i(\Sigma_{ii}^*)\, 8(1 + 4\sigma^2)\right]^{-1}$ and $f(n, \delta) = (1/4)\exp(c_* n\delta^2)$, where $c_* = \left[128(1 + 4\sigma^2)^2 \max_i(\Sigma_{ii}^*)^2\right]^{-1}$. As a consequence, for this particular model, the inverse functions $\bar{\delta}_f(n, p^\tau)$ and $\bar{n}_f(\delta, p^\tau)$ take the form

$$\bar{\delta}_f(n, p^\tau) \;=\; \sqrt{\frac{\log(4\,p^\tau)}{c_*\, n}} \;=\; \sqrt{128(1 + 4\sigma^2)^2 \max_i(\Sigma_{ii}^*)^2}\, \sqrt{\frac{\tau \log p + \log 4}{n}}, \quad \text{and} \tag{32a}$$

$$\bar{n}_f(\delta, p^\tau) \;=\; \frac{\log(4\,p^\tau)}{c_*\delta^2} \;=\; 128(1 + 4\sigma^2)^2 \max_i(\Sigma_{ii}^*)^2 \left(\frac{\tau \log p + \log 4}{\delta^2}\right). \tag{32b}$$

Substituting these forms into the claim of Theorem 1 and doing some simple algebra yields the stated corollary. □

When $\kappa_{\Gamma^*}, \kappa_{\Sigma^*}, \alpha$ remain constant as a function of (n, p, d), the corollary can be summarized succinctly as a sample size of $n = \Omega(d^2 \log p)$ samples ensures that an elementwise ℓ_∞ bound $\|\widehat{\Theta} - \Theta^*\|_\infty = \mathcal{O}\left(\sqrt{\frac{\log p}{n}}\right)$ holds with high probability. In practice, one frequently considers graphs with maximum node degrees d that either remain bounded, or that grow sub-linearly with the graph size (i.e., $d = o(p)$). In such cases, the sample size allowed by the corollary can be substantially smaller than the graph size, so that for sub-Gaussian random variables, the method can succeed in the $p \gg n$ regime.

3.2.2. Polynomial-type tails

We now state a corollary for the case of a polynomial-type tail function, such as those ensured by the case of random variables with appropriately bounded moments.

Corollary 2. *Under the assumptions of Theorem 1, suppose the rescaled variables $X_i/\sqrt{\Sigma_{ii}^*}$ have $4m^{th}$ moments upper bounded by K_m, and the sampling is i.i.d. Then if the sample size n satisfies the bound*

$$n \quad > \quad C_2 \, d^2 \left(1 + \frac{8}{\alpha}\right)^2 p^{\tau/m}, \tag{33}$$

where $C_2 := \left\{ 12m \left[m(K_m+1) \right]^{\frac{1}{2m}} \max_i (\Sigma_{ii}^*) \max\{ \kappa_{\Sigma^*}^2 \kappa_{\Gamma^*}, \kappa_{\Sigma^*}^4 \kappa_{\Gamma^*}^2 \} \right\}^2$, then with probability greater than $1 - 1/p^{\tau-2}$, the estimate $\widehat{\Theta}$ satisfies the bound,

$$\|\widehat{\Theta} - \Theta^*\|_\infty \;\leq\; \left\{ 4m[m(K_m+1)]^{\frac{1}{2m}} \left(1 + \frac{8}{\alpha}\right) \kappa_{\Gamma^*} \right\} \sqrt{\frac{p^{\tau/m}}{n}}.$$

Proof. Recall from Lemma 2 that when the rescaled variables $X_i/\sqrt{\Sigma_{ii}^*}$ have bounded $4m^{th}$ moments, then the sample covariance $\widehat{\Sigma}$ satisfies the tail condition $\mathcal{T}(f, v_*)$ with $v_* = 0$, and with $f(n,\delta) = c_* n^m \delta^{2m}$ with c_* defined as $c_* = 1/\left\{ m^{2m+1} 2^{2m} (\max_i \Sigma_{ii}^*)^{2m} (K_m + 1) \right\}$. As a consequence, for this particular model, the inverse functions take the form

$$\bar{\delta}_f(n, p^\tau) \;=\; \frac{(p^\tau/c_*)^{1/2m}}{\sqrt{n}} \;=\; \left\{ 2m[m(K_m+1)]^{\frac{1}{2m}} \max_i \Sigma_{ii}^* \right\} \sqrt{\frac{p^{\tau/m}}{n}}, \quad \text{and} \tag{34a}$$

$$\bar{n}_f(\delta, p^\tau) \;=\; \frac{(p^\tau/c_*)^{1/m}}{\delta^2} \;=\; \left\{ 2m[m(K_m+1)]^{\frac{1}{2m}} \max_i \Sigma_{ii}^* \right\}^2 \left(\frac{p^{\tau/m}}{\delta^2} \right). \tag{34b}$$

The claim then follows by substituting these expressions into Theorem 1 and performing some algebra. □

When the quantities $(\kappa_{\Gamma^*}, \kappa_{\Sigma^*}, \alpha)$ remain constant as a function of (n, p, d), Corollary 2 can be summarized succinctly as $n = \Omega(d^2 p^{\tau/m})$ samples are sufficient to achieve a convergence rate in elementwise ℓ_∞-norm of the order $\|\widehat{\Theta} - \Theta^*\|_\infty = \mathcal{O}\left(\sqrt{\frac{p^{\tau/m}}{n}}\right)$, with high probability. Consequently, both the required sample size and the rate of convergence of the estimator are polynomial in the number of variables p. It is worth contrasting these rates with the case of sub-Gaussian random variables, where the rates have only logarithmic dependence on the problem size p.

3.3. Model selection consistency

Part (b) of Theorem 1 asserts that the edge set $E(\widehat{\Theta})$ returned by the estimator is contained within the true edge set $E(\Theta^*)$—meaning that it correctly *excludes* all non-edges—and that it includes all edges that are "large" relative to the $\bar{\delta}_f(n, p^\tau)$ decay of the error. The following result, essentially a minor refinement of Theorem 1, provides sufficient conditions linking the sample size n and the minimum value

$$\theta_{\min} \;:=\; \min_{(i,j) \in E(\Theta^*)} |\Theta_{ij}^*| \tag{35}$$

for model selection consistency. More precisely, define the event

$$\mathcal{M}(\widehat{\Theta}; \Theta^*) \;:=\; \left\{ \operatorname{sign}(\widehat{\Theta}_{ij}) = \operatorname{sign}(\Theta_{ij}^*) \quad \forall (i,j) \in E(\Theta^*) \right\} \tag{36}$$

that the estimator $\widehat{\Theta}$ has the same edge set as Θ^*, and moreover recovers the correct signs on these edges. With this notation, we have:

Theorem 2. *Under the same conditions as Theorem 1, suppose that the sample size satisfies the lower bound*

$$n > \bar{n}_f \left(1 / \max \left\{ 2\kappa_{\Gamma^*} (1 + 8\alpha^{-1}) \, \theta_{\min}^{-1}, v_*, \right.\right.$$

$$\left.\left. 6(1 + 8\alpha^{-1}) \, d \, \max\{\kappa_{\Sigma^*} \kappa_{\Gamma^*}, \kappa_{\Sigma^*}^3 \kappa_{\Gamma^*}^2\} \right\}, p^\tau \right). \tag{37}$$

Then the estimator is model selection consistent with high probability as $p \to \infty$,

$$\mathbb{P}\big[\mathcal{M}(\widehat{\Theta}; \Theta^*)\big] \geq 1 - 1/p^{\tau-2} \to 1. \tag{38}$$

In comparison to Theorem 1, the sample size requirement (37) differs only in the additional term $\frac{2\kappa_{\Gamma^*}(1+\frac{8}{\alpha})}{\theta_{\min}}$ involving the minimum value. This term can be viewed as constraining how quickly the minimum can decay as a function of (n, p), as we illustrate with some concrete tail functions.

3.3.1. Exponential-type tails

Recall the setting of Section 2.3.1, where the random variables $\{X_i^{(k)}/\sqrt{\Sigma_{ii}^*}\}$ are sub-Gaussian with parameter σ. Let us suppose that the parameters $(\kappa_{\Gamma^*}, \kappa_{\Sigma^*}, \alpha)$ are viewed as constants (not scaling with (p, d). Then, using the expression (32) for the inverse function $\bar{n}_f$ in this setting, a corollary of Theorem 2 is that a sample size

$$n = \Omega\big((d^2 + \theta_{\min}^{-2}) \, \tau \log p\big) \tag{39}$$

is sufficient for model selection consistency with probability greater than $1 - 1/p^{\tau-2}$. Alternatively, we can state that $n = \Omega(\tau d^2 \log p)$ samples are sufficient, as along as the minimum value scales as $\theta_{\min} = \Omega(\sqrt{\frac{\log p}{n}})$.

3.3.2. Polynomial-type tails

Recall the setting of Section 2.3.2, where the rescaled random variables $X_i/\sqrt{\Sigma_{ii}^*}$ have bounded $4m^{th}$ moments. Using the expression (34) for the inverse function $\bar{n}_f$ in this setting, a corollary of Theorem 2 is that a sample size

$$n = \Omega\big((d^2 + \theta_{\min}^{-2}) \, p^{\tau/m}\big) \tag{40}$$

is sufficient for model selection consistency with probability greater than $1 - 1/p^{\tau-2}$. Alternatively, we can state than $n = \Omega(d^2 p^{\tau/m})$ samples are sufficient, as long as the minimum value scales as $\theta_{\min} = \Omega(p^{\tau/(2m)}/\sqrt{n})$.

3.4. Rates in Frobenius and spectral norm

We now derive some corollaries of Theorem 1 concerning estimation of Θ^* in Frobenius norm, as well as the spectral norm. Recall that $s = |E(\Theta^*)|$ denotes the total number of off-diagonal non-zeros in Θ^*.

Corollary 3. *Under the same assumptions as Theorem 1, with probability at least $1 - 1/p^{\tau-2}$, the estimator $\widehat{\Theta}$ satisfies*

$$\|\widehat{\Theta} - \Theta^*\|_F \leq \left\{ 2\kappa_{\Gamma^*}\left(1 + \frac{8}{\alpha}\right) \right\} \sqrt{s+p}\; \bar{\delta}_f(n, p^\tau), \qquad and \qquad (41a)$$

$$\|\widehat{\Theta} - \Theta^*\|_2 \leq \left\{ 2\kappa_{\Gamma^*}\left(1 + \frac{8}{\alpha}\right) \right\} \min\{\sqrt{s+p},\, d\}\; \bar{\delta}_f(n, p^\tau). \qquad (41b)$$

Proof. With the shorthand notation $\nu := 2\kappa_{\Gamma^*}(1 + 8/\alpha)\; \bar{\delta}_f(n, p^\tau)$, Theorem 1 guarantees that, with probability at least $1 - 1/p^{\tau-2}$, $\|\widehat{\Theta} - \Theta^*\|_\infty \leq \nu$. Since the edge set of $\widehat{\Theta}$ is a subset of that of Θ^*, and Θ^* has at most $p + s$ non-zeros (including the diagonal elements), we conclude that

$$\|\widehat{\Theta} - \Theta^*\|_F = \left[\sum_{i=1}^{p}(\widehat{\Theta}_{ii} - \Theta_{ii}^*)^2 + \sum_{(i,j)\in E} (\widehat{\Theta}_{ij} - \Theta_{ij}^*)^2 \right]^{1/2}$$

$$\leq \nu\,\sqrt{s+p},$$

from which the bound (41a) follows. On the other hand, for a symmetric matrix, we have

$$\|\widehat{\Theta} - \Theta^*\|_2 \leq \|\widehat{\Theta} - \Theta^*\|_\infty \leq d\nu, \qquad (42)$$

using the definition of the ν_∞-operator norm, and the fact that $\widehat{\Theta}$ and Θ^* have at most d non-zeros per row. Since the Frobenius norm upper bounds the spectral norm, the bound (41b) follows. $\square$

3.4.1. Exponential-type tails

For the exponential tail function case where the rescaled random variables $X_i/\sqrt{\Sigma_{ii}^*}$ are sub-Gaussian with parameter σ, we can use the expression (32) for the inverse function $\bar{\delta}_f$ to derive rates in Frobenius and spectral norms. When the quantities $\kappa_{\Gamma^*}, \kappa_{\Sigma^*}, \alpha$ remain constant, these bounds can be summarized succinctly as a sample size $n = \Omega(d^2 \log p)$ is sufficient to guarantee the bounds

$$\|\widehat{\Theta} - \Theta^*\|_F = \mathcal{O}\left(\sqrt{\frac{(s+p)\,\log p}{n}}\right), \quad and \qquad (43a)$$

$$\|\widehat{\Theta} - \Theta^*\|_2 = \mathcal{O}\left(\sqrt{\frac{\min\{s+p,\, d^2\}\,\log p}{n}}\right), \qquad (43b)$$

with probability at least $1 - 1/p^{\tau-2}$.

3.4.2. Polynomial-type tails

Similarly, let us again consider the polynomial tail case, in which the rescaled variates $X_i/\sqrt{\Sigma_{ii}^*}$ have bounded $4m^{th}$ moments and the samples are drawn i.i.d. Using the expression (34) for the inverse function we can derive rates in the Frobenius and spectral norms. When the quantities $\kappa_{\Gamma^*}, \kappa_{\Sigma^*}, \alpha$ are viewed as constant, we are guaranteed that a sample size $n = \Omega(d^2\, p^{\tau/m})$ is sufficient to guarantee the bounds

$$\|\widehat{\Theta} - \Theta^*\|_F = \mathcal{O}\left(\sqrt{\frac{(s+p)\,p^{\tau/m}}{n}}\right), \text{ and} \tag{44a}$$

$$\|\widehat{\Theta} - \Theta^*\|_2 = \mathcal{O}\left(\sqrt{\frac{\min\{s+p,\, d^2\}\,p^{\tau/m}}{n}}\right), \tag{44b}$$

with probability at least $1 - 1/p^{\tau-2}$.

Remark It is worth observing that our results also have implications for estimating the covariance matrix Σ^* in operator norm. By Lemma 3, the estimated concentration matrix $\widehat{\Theta}$ is positive definite, and hence can be inverted to obtain an estimate of the covariance matrix, and we state explicit rates in Corollary 4 on pp. 15 of our extended tech-report [25]. These rates are equivalent to those obtained by and Levina [1] and El Karoui [10] for thresholding estimators, as applied to sparse *covariance matrices*, whereas our rates are applicable to sparse *inverse covariance* matrices.

3.5. Comparisons to other results

In this section, we compare our results against those in some related work.

3.5.1. Comparison to neighbor-based graphical model selection

Suppose that X follows a multivariate Gaussian distribution, so that the structure of the concentration matrix Θ^* specifies the structure of a Gaussian graphical model. In this case, the neighborhood-based method, first proposed by Meinshausen and Bühlmann [22], estimates the full graph structure by performing an ℓ_1-regularized linear regression (Lasso)—of the form $X_i = \sum_{j \neq i} \theta_{ij} X_j + W$— of each node on its neighbors and using the support of the estimated regression vector θ to predict the neighborhood set. These neighborhoods are then combined, by either an OR rule or an AND rule, to estimate the full graph. It is interesting to compare our conditions for graphical model consistency of the log-determinant approach, as specified in Theorem 2, to those of the Lasso based neighborhood selection method. Various aspects of the high-dimensional model selection consistency of the Lasso are now understood [22, 29, 32]. It is known that mutual incoherence or irrepresentability conditions are necessary

and sufficient for its success [28, 32]. In terms of scaling, Wainwright [29] shows that the Lasso succeeds with high probability if and only if the sample size scales as $n \asymp c(\{d + \theta_{\min}^{-2}\} \log p)$, assuming sub-Gaussian noise where c is a constant determined by the covariance matrix Σ^*. By a union bound over the p nodes in the graph, it then follows that the neighbor-based graph selection method in turn succeeds with high probability if $n = \Omega(\{d + \theta_{\min}^{-2}\} \log p)$.

For comparison, consider the application of Theorem 2 to the case where the variables are sub-Gaussian (which includes the Gaussian case). For this setting, we have seen that the scaling required by Theorem 2 is $n = \Omega(\{d^2 + \theta_{\min}^{-2}\} \log p)$, so that the dependence of the log-determinant approach on $\theta_{\min}$ is identical, but it depends quadratically on the maximum degree d. We suspect that that the quadratic dependence d^2 might be an artifact of our analysis, but have not yet been able to reduce it to d. Otherwise, the primary difference between the two methods is in the nature of the irrepresentability assumptions that are imposed: our method requires Assumption 1 on the Hessian Γ^*, whereas the neighborhood-based method imposes the same type of condition on a set of p covariance matrices, each of size $(p-1) \times (p-1)$, one for each node of the graph. In section 3.1.2 we showed two cases where the Lasso irrepresentability condition holds, while the log-determinant requirement fails. However, in general, we do not know whether the log-determinant irrepresentability strictly is more restrictive than its analog for the Lasso.

3.5.2. Comparison to past work

We now discuss in some detail the differences between our result and past work [18, 27]. In the first paper to analyze high-dimensional aspects of the log-determinant estimator (11), Rothman et al. [27] consider the case of multivariate Gaussian data, in which case the estimator coincides with the ℓ_1 regularized Gaussian MLE. In this setting, they obtained convergence rates in Frobenius norm of $\|\widehat{\Theta} - \Theta^*\|_F = \mathcal{O}\big(\sqrt{\frac{(s+p)\log p}{n}}\big)$. Since the Frobenius norm upper bounds the spectral norm, they also obtained the same convergence rate for the spectral norm. In this paper, for variables with sub-Gaussian tails, we obtained convergence in spectral norm at the rate $\mathcal{O}\big(\sqrt{\frac{\min\{d^2, (s+p)\} \log p}{n}}\big)$, where d denotes the maximum number of non-zeros per row (or the maximum degree of the graph). For graphs with degrees that do not grow too quickly (i.e., under the inequality $d^2 \leq s + p$, which holds for bounded degree graphs among others), then the rate obtained here is faster. To be clear, the Rothman et al. [27] analysis involved milder restrictions on the inverse covariance, namely only a lower bound on its eigenvalues, whereas our results (since they were derived via model selection consistency) required stronger conditions on the matrix and its incoherence properties (via the parameters κ_{Γ^*} and κ_{Σ^*} and α). On the other hand, the analysis of this paper applies somewhat more generally to random vectors with tail behavior other than sub-Gaussian, where we obtained different rates depending on the heaviness of the tails.

In addition, Rothman et al. [27] proposed a slightly different estimator than (11) for the multivariate Gaussian case: they first estimate the correlation matrix by solving the program (11) with the sample correlation matrix substituted in place of the sample covariance matrix, and use this to obtain an estimate of the concentration matrix. They obtained a an improved ℓ_2 operator norm convergence rate for this estimator—namely, $\|\widehat{\Theta} - \Theta^*\|_2 = \mathcal{O}\big(\sqrt{\frac{(s+1)\log p}{n}}\big)$—which is better when $s \ll p$. Although this yields improvements for very sparse graphs, for any connected graph, the number of edges scales as $s = \Omega(p)$, in which case it is not substantially better than the ordinary estimator. Nonetheless, it would be interesting to extend our analysis to their "improved" estimator to see if one could improve the bound in (43b).

In subsequent work, Lam and Fan [18] proposed a generalization of the log-determinant estimator (11) involving more general regularization functions. Most germane to this discussion are their results for ℓ_1-regularization, in which case their estimator is equivalent to the log-determinant estimator (11), and their Frobenius and ℓ_2 operator norm convergence rates match those in Rothman et al. [27]. In addition, Lam and Fan [18] provide a result on model-selection consistency of the estimator (11), but one which needs fairly restrictive conditions on the sparsity of the graph and the sample size. In particular, they require that the number of edges s be upper bounded as $s = \mathcal{O}(\sqrt{p})$, and that the sample size be lower bounded as $n = \Omega((s+p)\log p)$. Note that the first condition limits their result to graphs that are very sparse, in particular excluding any connected graph, or any graph with constant node degrees d (for which $s = dp/2$). Additionally, the lower bound on the sample size implies that consistency cannot be obtained in the high-dimensional setting with $p \gg n$. In contrast, we guarantee model selection consistency with sample size $n = \Omega(d^2 \log p)$, which allows for connected graphs and constant degree graphs as well as for high-dimensional scaling. Note that our result is based on the incoherence condition imposed in Assumption 1.

4. Proofs of main result

In this section, we work through the proofs of Theorems 1 and 2. We break down the proofs into a sequence of lemmas, with some of the more technical aspects deferred to appendices. Our proofs are based on a technique that we call a *primal-dual witness method*, used previously in analysis of the Lasso [29]. It involves following a specific sequence of steps to construct a pair $(\widetilde{\Theta}, \widetilde{Z})$ of symmetric matrices that together satisfy the optimality conditions associated with the convex program (11) *with high probability*. Thus, when the constructive procedure succeeds, $\widetilde{\Theta}$ is *equal* to the unique solution $\widehat{\Theta}$ of the convex program (11), and $\widetilde{Z}$ is an optimal solution to its dual. In this way, the estimator $\widehat{\Theta}$ inherits from $\widetilde{\Theta}$ various optimality properties in terms of its distance to the truth Θ^*, and its recovery of the signed sparsity pattern. To be clear, our procedure for constructing $\widetilde{\Theta}$ is *not* a practical algorithm for solving the log-determinant

problem (11), but rather is used as a proof technique for certifying the behavior of the M-estimator (11).

4.1. Primal-dual witness approach

As outlined above, at the core of the primal-dual witness method are the standard convex optimality conditions that characterize the optimum $\widehat{\Theta}$ of the convex program (11). For future reference, we note that the sub-differential of the norm $\|\cdot\|_{1,\text{off}}$ evaluated at some Θ consists the set of all symmetric matrices $Z \in \mathbb{R}^{p \times p}$ such that

$$
Z_{ij} \;\; = \;\; \begin{cases} 0 & \text{if } i = j \\ \text{sign}(\Theta_{ij}) & \text{if } i \neq j \text{ and } \Theta_{ij} \neq 0 \\ \in [-1, +1] & \text{if } i \neq j \text{ and } \Theta_{ij} = 0. \end{cases} \tag{45}
$$

The following result is proved in Appendix A:

Lemma 3. *For any $\lambda_n > 0$ and sample covariance $\widehat{\Sigma}$ with strictly positive diagonal elements, the ℓ_1-regularized log-determinant problem (11) has a unique solution $\widehat{\Theta} \succ 0$ characterized by*

$$
\widehat{\Sigma} - \widehat{\Theta}^{-1} + \lambda_n \widehat{Z} \;\; = \;\; 0, \tag{46}
$$

where $\widehat{Z}$ is an element of the subdifferential $\partial\|\widehat{\Theta}\|_{1,\text{off}}$.

Based on this lemma, we construct the primal-dual witness solution $(\widetilde{\Theta}, \widetilde{Z})$ as follows:

(a) We determine the matrix $\widetilde{\Theta}$ by solving the restricted log-determinant problem

$$
\widetilde{\Theta} \;\; := \;\; \arg\min_{\Theta \succ 0, \Theta = \Theta^T, \, \Theta_{S^c} = 0} \big\{ \langle\!\langle \Theta, \, \widehat{\Sigma} \rangle\!\rangle - \log\det(\Theta) + \lambda_n \|\Theta\|_{1,\text{off}} \big\}. \tag{47}
$$

Note that by construction, we have $\widetilde{\Theta} \succ 0$, and moreover $\widetilde{\Theta}_{S^c} = 0$.

(b) We choose $\widetilde{Z}$ as a member of the sub-differential of the regularizer $\|\cdot\|_{1,\text{off}}$, evaluated at $\widetilde{\Theta}$.

(c) For each $(i, j) \in S^c$, we replace $\widetilde{Z}_{ij}$ with the quantity

$$
\widetilde{Z}_{ij} \;\; := \;\; \frac{1}{\lambda_n}\big\{ -\widehat{\Sigma}_{ij} + [\widetilde{\Theta}^{-1}]_{ij} \big\}, \tag{48}
$$

which ensures that constructed matrices $(\widetilde{\Theta}, \widetilde{Z})$ satisfy the optimality condition (46).

(d) We verify the *strict dual feasibility* condition

$$
|\widetilde{Z}_{ij}| \;\; < \;\; 1 \quad \text{for all } (i, j) \in S^c.
$$

To clarify the nature of the construction, steps (a) through (c) suffice to obtain a pair $(\widetilde{\Theta}, \widetilde{Z})$ that satisfy the optimality conditions (46), but do *not* guarantee that $\widetilde{Z}$ is an element of the sub-differential $\partial\|\widetilde{\Theta}\|_{1,\text{off}}$. By construction, specifically step (b) of the construction ensures that the entries $\widetilde{Z}$ in S satisfy the sub-differential conditions, since $\widetilde{Z}_S$ is a member of the sub-differential $[\partial\|\widetilde{\Theta}\|_{1,\text{off}}]_S$. The purpose of step (d), then, is to verify that the remaining elements of $\widetilde{Z}$ satisfy the necessary conditions to belong to the sub-differential.

If the primal-dual witness construction succeeds, then it acts as a *witness* to the fact that the solution $\widetilde{\Theta}$ to the restricted problem (47) is equal to the solution $\widehat{\Theta}$ to the original (unrestricted) problem (11). We exploit this fact in our proofs of Theorems 1 and 2 that build on this: we first show that the primal-dual witness technique succeeds with high-probability, from which we can conclude that the support of the optimal solution $\widehat{\Theta}$ is contained within the support of the true Θ^*. In addition, we exploit the characterization of $\widehat{\Theta}$ provided by the primal-dual witness construction to establish the elementwise ℓ_∞ bounds claimed in Theorem 1. Theorem 2 requires checking, in addition, that certain sign consistency conditions hold, for which we require lower bounds on the value of the minimum value $\theta_{\min}$. Note that if (d) fails then the converse holds and we can conclude that the support of the optimal solution $\widehat{\Theta}$ is not contained within the support of the true Θ^*. This claim follows from uniqueness of the solution $\widehat{\Theta}$, and the fact that any solution of the convex program (11) must satisfy the stationary condition (46).

In the analysis to follow, some additional notation is useful. We let $W \in \mathbb{R}^{p \times p}$ denote the "effective noise" in the sample covariance matrix $\widehat{\Sigma}$—namely, the quantity

$$W \quad := \quad \widehat{\Sigma} - (\Theta^*)^{-1}. \tag{49}$$

Second, we use $\Delta = \widetilde{\Theta} - \Theta^*$ to measure the discrepancy between the primal witness matrix $\widetilde{\Theta}$ and the truth Θ^*. Note that by the definition of $\widetilde{\Theta}$, $\Delta_{S^c} = 0$. Finally, recall the log-determinant barrier g from equation (6). We let $R(\Delta)$ denote the difference of the gradient $\nabla g(\widetilde{\Theta}) = \widetilde{\Theta}^{-1}$ from its first-order Taylor expansion around Θ^*. Using known results on the first and second derivatives of the log-determinant function (see p. 641 in Boyd and Vandenberghe [3]), this remainder takes the form

$$R(\Delta) \quad = \quad \widetilde{\Theta}^{-1} - \Theta^{*-1} + \Theta^{*-1}\Delta\Theta^{*-1}. \tag{50}$$

4.2. Auxiliary results

We begin with some auxiliary lemmata, required in the proofs of our main theorems. In Section 4.2.1, we provide sufficient conditions on the quantities W and R for the strict dual feasibility condition to hold. In Section 4.2.2, we control the remainder term $R(\Delta)$ in terms of Δ, while in Section 4.2.3, we control Δ

itself, providing elementwise ℓ_∞ bounds on Δ. In Section 4.2.4, we show that under appropriate conditions on the minimum value $\theta_{\min}$, the bounds in the earlier lemmas guarantee that the sign consistency condition holds. All of the analysis in these sections is *deterministic* in nature. In Section 4.2.5, we turn to the probabilistic component of the analysis, providing control of the noise W in the sample covariance matrix. Finally, the proofs of Theorems 1 and 2 follows by using this probabilistic control of W and the stated conditions on the sample size to show that the deterministic conditions hold with high probability.

4.2.1. Sufficient conditions for strict dual feasibility

We begin by stating and proving a lemma that provides sufficient condition for strict dual feasibility to hold, so that $\|\widetilde{Z}_{S^c}\|_\infty < 1$.

Lemma 4 (Strict dual feasibility). *Suppose that*

$$\max\left\{\|W\|_\infty,\ \|R(\Delta)\|_\infty\right\} \ \le\ \frac{\alpha\,\lambda_n}{8}. \tag{51}$$

Then the vector $\widetilde{Z}_{S^c}$ constructed in step (c) satisfies $\|\widetilde{Z}_{S^c}\|_\infty < 1$, and therefore $\widetilde{\Theta} = \widehat{\Theta}$.

Proof. Using the definitions (49) and (50), we can re-write the stationary condition (46) in an alternative but equivalent form

$$\Theta^{*-1}\Delta\Theta^{*-1} + W - R(\Delta) + \lambda_n\widetilde{Z} \ = 0. \tag{52}$$

This is a linear-matrix equality, which can be re-written as an ordinary linear equation by "vectorizing" the matrices. We use the notation $\mathrm{vec}(A)$, or equivalently $\overline{A}$ for the vector version of the set or matrix A obtained by stacking up the rows of A into a single column vector.

$$\mathrm{vec}\left(\Theta^{*-1}\Delta\Theta^{*-1}\right) = \left(\Theta^{*-1}\otimes\Theta^{*-1}\right)\overline{\Delta} \ = \ \Gamma^*\overline{\Delta}.$$

In terms of the disjoint decomposition S and S^c, equation (52) can be re-written as two blocks of linear equations as follows:

$$\Gamma^*_{SS}\overline{\Delta}_S + \overline{W}_S - \overline{R}_S + \lambda_n\overline{\widetilde{Z}}_S \ = \ 0 \tag{53a}$$

$$\Gamma^*_{S^cS}\overline{\Delta}_S + \overline{W}_{S^c} - \overline{R}_{S^c} + \lambda_n\overline{\widetilde{Z}}_{S^c} \ = \ 0. \tag{53b}$$

Here we have used the fact that $\Delta_{S^c} = 0$ by construction.

Since Γ^*_{SS} is invertible, we can solve for $\overline{\Delta}_S$ from equation (53a) as follows:

$$\overline{\Delta}_S \ = \ \left(\Gamma^*_{SS}\right)^{-1}\left[-\overline{W}_S + \overline{R}_S - \lambda_n\overline{\widetilde{Z}}_S\right].$$

Substituting this expression into equation (53b), we can solve for $\widetilde{Z}_{S^c}$ as follows:

$$
\begin{aligned}
\bar{\bar{Z}}_{S^c} &= -\frac{1}{\lambda_n}\Gamma^*_{S^c S}\bar{\Delta}_S + \frac{1}{\lambda_n}\bar{R}_{S^c} - \frac{1}{\lambda_n}\bar{W}_{S^c} \\
&= -\frac{1}{\lambda_n}\Gamma^*_{S^c S}\left(\Gamma^*_{SS}\right)^{-1}(\bar{W}_S - \bar{R}_S) + \Gamma^*_{S^c S}\left(\Gamma^*_{SS}\right)^{-1}\bar{\bar{Z}}_S \\
&\quad - \frac{1}{\lambda_n}(\bar{W}_{S^c} - \bar{R}_{S^c}).
\end{aligned}
\tag{54}
$$

Taking the ℓ_∞ norm of both sides yields

$$
\begin{aligned}
\|\bar{\bar{Z}}_{S^c}\|_\infty \leq &\frac{1}{\lambda_n}\|\Gamma^*_{S^c S}\left(\Gamma^*_{SS}\right)^{-1}\|_\infty(\|\bar{W}_S\|_\infty + \|\bar{R}_S\|_\infty) \\
&+ \|\Gamma^*_{S^c S}\left(\Gamma^*_{SS}\right)^{-1}\bar{\bar{Z}}_S\|_\infty + \frac{1}{\lambda_n}(\|\bar{W}_S\|_\infty + \|\bar{R}_S\|_\infty).
\end{aligned}
$$

Recalling Assumption 1, we obtain that $\|\Gamma^*_{S^c S}\left(\Gamma^*_{SS}\right)^{-1}\bar{\bar{Z}}_{S^c}\|_\infty \leq (1-\alpha)$, so that we have

$$
\|\bar{\bar{Z}}_{S^c}\|_\infty \ \leq \ \frac{2-\alpha}{\lambda_n}\left(\|\bar{W}_S\|_\infty + \|\bar{R}_S\|_\infty\right) + (1-\alpha),
\tag{55}
$$

where we have used the fact that $\|\bar{\bar{Z}}_S\|_\infty \leq 1$, since $\widetilde{Z}$ belongs to the sub-differential of the norm $\|\cdot\|_{1,\mathrm{off}}$ by construction. Finally, applying assumption (51) from the lemma statement, we have

$$
\|\bar{\bar{Z}}_{S^c}\|_\infty \ \leq \ \frac{(2-\alpha)}{\lambda_n}\left(\frac{\alpha\lambda_n}{4}\right) + (1-\alpha) \ \leq \ \frac{\alpha}{2} + (1-\alpha) \ < \ 1,
$$

as claimed. $\square$

4.2.2. Control of remainder term

Our next step is to relate the behavior of the remainder term (50) to the deviation $\Delta = \widetilde{\Theta} - \Theta^*$.

Lemma 5 (Control of remainder). *Suppose that the elementwise ℓ_∞-bound $\|\Delta\|_\infty \leq \frac{1}{3\kappa_{\Sigma^*}d}$ holds. Then the matrix $J := \sum_{k=0}^\infty (-1)^k\left(\Theta^{*-1}\Delta\right)^k$ satisfies the ℓ_∞-operator norm $\|J^T\|_\infty \leq 3/2$, and moreover, the matrix*

$$
R(\Delta) \ = \ \Theta^{*-1}\Delta\Theta^{*-1}\Delta J\Theta^{*-1},
\tag{56}
$$

has elementwise ℓ_∞-norm bounded as

$$
\|R(\Delta)\|_\infty \ \leq \ \frac{3}{2}d\|\Delta\|_\infty^2\,\kappa_{\Sigma^*}^3.
\tag{57}
$$

We provide the proof of this lemma in Appendix B using matrix expansion techniques.

4.2.3. Sufficient conditions for ℓ_∞ bounds

Our next lemma provides control on the deviation $\Delta = \widetilde{\Theta} - \Theta^*$, measured in elementwise ℓ_∞ norm.

Lemma 6 (Control of Δ). *Suppose that*

$$r := 2\kappa_{\Gamma^*}\big(\|W\|_\infty + \lambda_n\big) \quad \leq \quad \min\left\{\frac{1}{3\kappa_{\Sigma^*}d},\ \frac{1}{3\kappa_{\Sigma^*}^3\ \kappa_{\Gamma^*}d}\right\}. \tag{58}$$

Then we have the elementwise ℓ_∞ bound

$$\|\Delta\|_\infty = \|\widetilde{\Theta} - \Theta^*\|_\infty \quad \leq \quad r. \tag{59}$$

We prove the lemma in Appendix C; at a high level, the main steps involved are the following. We begin by noting that $\widetilde{\Theta}_{S^c} = \Theta^*_{S^c} = 0$, so that $\|\Delta\|_\infty = \|\Delta_S\|_\infty$. Next, we characterize $\widetilde{\Theta}_S$ in terms of the zero-gradient condition associated with the restricted problem (47). We then define a continuous map $F : \Delta_S \mapsto F(\Delta_S)$ such that its fixed points are equivalent to zeros of this gradient expression in terms of $\Delta_S = \widetilde{\Theta}_S - \Theta^*_S$. We then show that the function F maps the ℓ_∞-ball

$$\mathbb{B}(r) \quad := \quad \{\Theta_S \mid \|\Theta_S\|_\infty \leq r\}, \qquad \text{with } r := 2\kappa_{\Gamma^*}\big(\|W\|_\infty + \lambda_n\big), \tag{60}$$

onto itself. Finally, with these results in place, we can apply Brouwer's fixed point theorem (e.g., p. 161; Ortega and Rheinboldt [23]) to conclude that F does indeed have a fixed point inside $\mathbb{B}(r)$.

4.2.4. Sufficient conditions for sign consistency

A lower bound on the minimum value $\theta_{\min}$, when combined with Lemma 6 immediately yields a guarantee on the *sign consistency* of the primal witness matrix $\widetilde{\Theta}$.

Lemma 7 (Sign Consistency of Oracle Estimator $\widetilde{\Theta}$). *Suppose the conditions of Lemma 6 hold, and further that the minimum absolute value $\theta_{\min}$ of non-zero entries in the true concentration matrix Θ^* is lower bounded as*

$$\theta_{\min} \quad \geq \quad 4\kappa_{\Gamma^*}\big(\|W\|_\infty + \lambda_n\big), \tag{61}$$

then $sign(\widetilde{\Theta}_S) = sign(\Theta^*_S)$ holds.

Proof. From the bound (59), we have $|\widetilde{\Theta}_{ij} - \Theta^*_{ij}| \leq r,\ \forall(i,j) \in S$. Combining the definition (58) of r with the bound (61) on $\theta_{\min}$ yields that for all $(i,j) \in S$, the estimate $\widetilde{\Theta}_{ij}$ cannot differ enough from Θ^*_{ij} to change sign. $\qquad\square$

4.2.5. Control of noise term

The final ingredient required for the proofs of Theorems 1 and 2 is control on the sampling noise $W = \widehat{\Sigma} - \Sigma^*$. This control is specified in terms of the decay function f from equation (12).

Lemma 8 (Control of Sampling Noise). *For any $\tau > 2$ and sample size n such that $\bar{\delta}_f(n, p^\tau) \leq 1/v_*$, we have*

$$\mathbb{P}\left[\|W\|_\infty \geq \bar{\delta}_f(n, p^\tau) \right] \quad \leq \quad \frac{1}{p^{\tau-2}} \ \to \ 0. \tag{62}$$

Proof. Using the definition (12) of the decay function f, and applying the union bound over all p^2 entries of the noise matrix, we obtain that for all $\delta \leq 1/v_*$,

$$\mathbb{P}\left[\max_{i,j} |W_{ij}| \geq \delta \right] \quad \leq \quad p^2/f(n, \delta).$$

Setting $\delta = \bar{\delta}_f(n, p^\tau)$ yields that

$$\mathbb{P}\left[\max_{i,j} |W_{ij}| \geq \bar{\delta}_f(n, p^\tau) \right] \quad \leq \quad p^2 / \left[f(n, \bar{\delta}_f(n, p^\tau)) \right] \ = \ 1/p^{\tau-2},$$

as claimed. Here the last equality follows since $f(n, \bar{\delta}_f(n, p^\tau)) = p^\tau$, using the definition (14) of the inverse function $\bar{\delta}_f$.   □

4.3. Proof of Theorem 1

We now have the necessary ingredients to prove Theorem 1. We first show that with high probability the witness matrix $\widetilde{\Theta}$ is equal to the solution $\widehat{\Theta}$ to the original log-determinant problem (11), in particular by showing that the primal-dual witness construction (described in in Section 4.1) succeeds with high probability. Let $\mathcal{A}$ denote the event that $\|W\|_\infty \leq \bar{\delta}_f(n, p^\tau)$. Using the monotonicity of the inverse tail function (15), the lower lower bound (29) on the sample size n implies that $\bar{\delta}_f(n, p^\tau) \leq 1/v_*$. Consequently, Lemma 8 implies that $\mathbb{P}(\mathcal{A}) \geq 1 - \frac{1}{p^{\tau-2}}$. Accordingly, we condition on the event $\mathcal{A}$ in the analysis to follow.

We proceed by verifying that assumption (51) of Lemma 4 holds. Recalling the choice of regularization penalty $\lambda_n = (8/\alpha)\,\bar{\delta}_f(n, p^\tau)$, we have $\|W\|_\infty \leq (\alpha/8)\lambda_n$. In order to establish condition (51) it remains to establish the bound $\|R(\Delta)\|_\infty \leq \frac{\alpha \lambda_n}{8}$. We do so in two steps, by using Lemmas 6 and 5 consecutively. First, we show that the condition (58) required for Lemma 6 to hold is satisfied under the specified conditions on n and λ_n. From Lemma 8 and our choice of regularization constant $\lambda_n = (8/\alpha)\,\bar{\delta}_f(n, p^\tau)$,

$$2\kappa_{\Gamma^*}\left(\|W\|_\infty + \lambda_n \right) \quad \leq \quad 2\kappa_{\Gamma^*}\left(1 + \frac{8}{\alpha} \right) \bar{\delta}_f(n, p^\tau),$$

provided $\bar{\delta}_f(n, p^\tau) \leq 1/v_*$. From the lower bound (29) and the monotonicity (15) of the tail inverse functions, we have

$$2\kappa_{\Gamma^*}\left(1 + \frac{8}{\alpha}\right)\bar{\delta}_f(n, p^\tau) \;\leq\; \min\left\{\frac{1}{3\kappa_{\Sigma^*}d}, \; \frac{1}{3\kappa_{\Sigma^*}^3 \; \kappa_{\Gamma^*}d}\right\}, \tag{63}$$

showing that the assumptions of Lemma 6 are satisfied. Applying this lemma, we conclude that

$$\|\Delta\|_\infty \;\leq\; 2\kappa_{\Gamma^*}\big(\|W\|_\infty + \lambda_n\big) \;\leq\; 2\kappa_{\Gamma^*}\left(1 + \frac{8}{\alpha}\right)\bar{\delta}_f(n, p^\tau). \tag{64}$$

Turning next to Lemma 5, we see that its assumption $\|\Delta\|_\infty \leq \frac{1}{3\,\kappa_{\Sigma^*}d}$ holds, by applying equations (63) and (64). Consequently, we have

$$\begin{aligned}
\|R(\Delta)\|_\infty \;&\leq\; \frac{3}{2}\, d\, \|\Delta\|_\infty^2\, \kappa_{\Sigma^*}^3 \\
&\leq\; 6\kappa_{\Sigma^*}^3\kappa_{\Gamma^*}^2\, d\left(1 + \frac{8}{\alpha}\right)^2 [\bar{\delta}_f(n, p^\tau)]^2 \\
&=\; \left\{6\kappa_{\Sigma^*}^3\kappa_{\Gamma^*}^2\, d\left(1 + \frac{8}{\alpha}\right)^2 \bar{\delta}_f(n, p^\tau)\right\}\frac{\alpha\lambda_n}{8} \\
&\leq\; \frac{\alpha\lambda_n}{8},
\end{aligned}$$

as required, where the final inequality follows from our condition (29) on the sample size, and the monotonicity property (15).

Overall, we have shown that the assumption (51) of Lemma 4 holds, allowing us to conclude that $\widetilde{\Theta} = \widehat{\Theta}$. The estimator $\widehat{\Theta}$ then satisfies the ℓ_∞-bound (64) of $\widetilde{\Theta}$, as claimed in Theorem 1(a), and moreover, we have $\widehat{\Theta}_{S^c} = \widetilde{\Theta}_{S^c} = 0$, as claimed in Theorem 1(b). Since the above was conditioned on the event $\mathcal{A}$, these statements hold with probability $\mathbb{P}(\mathcal{A}) \geq 1 - \frac{1}{p^{\tau-2}}$.

4.4. *Proof of Theorem 2*

We now turn to the proof of Theorem 2. A little calculation shows that the assumed lower bound (37) on the sample size n and the monotonicity property (15) together guarantee that

$$\theta_{\min} \;>\; 4\kappa_{\Gamma^*}\left(1 + \frac{8}{\alpha}\right)\bar{\delta}_f(n, p^\tau)$$

Proceeding as in the proof of Theorem 1, with probability at least $1 - 1/p^{\tau-2}$, we have the equality $\widetilde{\Theta} = \widehat{\Theta}$, and also that $\|\widetilde{\Theta} - \Theta^*\|_\infty \leq \theta_{\min}/2$. Consequently, Lemma 7 can be applied, guaranteeing that $\mathrm{sign}(\Theta_{ij}^*) = \mathrm{sign}(\widetilde{\Theta}_{ij})$ for all $(i, j) \in E$. Overall, we conclude that with probability at least $1 - 1/p^{\tau-2}$, the sign consistency condition $\mathrm{sign}(\Theta_{ij}^*) = \mathrm{sign}(\widehat{\Theta}_{ij})$ holds for all $(i, j) \in E$, as claimed.
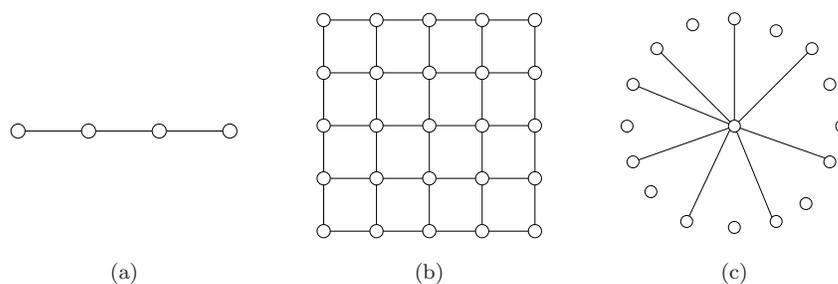
FIG 3. *Illustrations of different graph classes used in simulations. (a) Chain ($d = 2$). (b) Four-nearest neighbor grid ($d = 4$) and (c) Star-shaped graph ($d \in \{1, \ldots, p-1\}$).*

5. Experiments

In this section, we illustrate our results with various experimental simulations, reporting results in terms of the probability of correct model selection (Theorem 2) or the ℓ_∞-error (Theorem 1). For these illustrations, we study the case of Gaussian graphical models, and results for three different classes of graphs, namely chains, grids, and star-shaped graphs. In addition to varying the triple (n, p, d), we also report results concerning the role of the parameters κ_{Σ^*}, κ_{Γ^*} and $\theta_{\min}$ that we have identified in the main theorems. For all results reported here, we solved the resulting ℓ_1-penalized log-determinant program (11) using the glasso program of Friedman et al. [11], which builds on the block coordinate descent algorithm of d'Asprémont et al. [9].

Figure 3 illustrates the three types of graphs used in our simulations: chain graphs (panel (a)), four-nearest neighbor lattices or grids (panel (b)), and star-shaped graphs (panel (c)). For the chain and grid graphs, the maximal node degree d is fixed (by definition) to $d = 2$ for chains, and $d = 4$ for the grids. Consequently, these graphs can capture the dependence of the required sample size n only as a function of the graph size p, and the parameters (κ_{Σ^*}, κ_{Γ^*}, $\theta_{\min}$). The star graph allows us to vary both d and p, since the degree of the central hub can be varied between 1 and $p - 1$. For each graph type, we varied the size of the graph p in different ranges, from $p = 64$ upwards to $p = 375$.

For the chain and star graphs, we define a covariance matrix Σ^* with entries $\Sigma_{ii}^* = 1$ for all $i = 1, \ldots, p$, and $\Sigma_{ij}^* = \rho$ for all $(i, j) \in E$ for specific values of ρ specified below. Note that these covariance matrices are sufficient to specify the full model. For the four-nearest neighbor grid graph, we set the entries of the concentration matrix $\Theta_{ij}^* = \omega$ for $(i, j) \in E$, with the value ω specified below. In all cases, we set the regularization parameter λ_n proportional to $\sqrt{\log(p)/n}$, as suggested by Theorems 1 and 2, which is reasonable since the main purpose of these simulations is to illustrate our theoretical results. However, for general data sets, the relevant theoretical parameters cannot be computed (since the true model is unknown), so that a data-driven approach such as cross-validation might be required for selecting the regularization parameter λ_n.

Given a Gaussian graphical model instance, and the number of samples n, we drew $N = 100$ batches of n independent samples from the associated multivariate Gaussian distribution. We estimated the probability of correct model selection as the fraction of the $N = 100$ trials in which the estimator recovers the signed-edge set exactly.

Note that any multivariate Gaussian random vector is sub-Gaussian; in particular, the rescaled variates $X_i/\sqrt{\Sigma_{ii}^*}$ are sub-Gaussian with parameter $\sigma = 1$, so that the elementwise ℓ_∞-bound from Corollary 1 applies. Suppose we collect relevant parameters such as $\theta_{\min}$ and the covariance and Hessian-related terms κ_{Σ^*}, κ_{Γ^*} and α into a single "model-complexity" term K defined as

$$K \quad := \quad \left[(1 + 8\alpha^{-1})(\max_i \Sigma_{ii}^*) \max\left\{\kappa_{\Sigma^*}\kappa_{\Gamma^*}, \kappa_{\Sigma^*}^3\kappa_{\Gamma^*}^2, \frac{\kappa_{\Gamma^*}}{d\,\theta_{\min}}\right\}\right]. \quad (65)$$

Then, as a corollary of Theorem 2, a sample size of order

$$n \quad = \quad \Omega\left(K^2\,d^2\,\tau\log p\right), \quad (66)$$

is sufficient for model selection consistency with probability greater than $1 - 1/p^{\tau-2}$. In the subsections to follow, we investigate how the empirical sample size n required for model selection consistency scales in terms of graph size p, maximum degree d, as well as the "model-complexity" term K defined above.

5.1. Dependence on graph size

Panel (a) of Figure 4 plots the probability of correct signed edge-set recovery against the sample size n for a chain-structured graph of three different sizes. For these chain graphs, regardless of the number of nodes p, the maximum
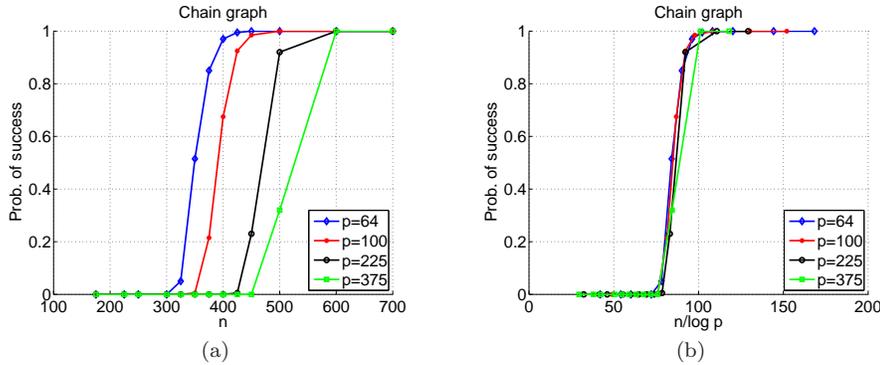

FIG 4. *Simulations for chain graphs with varying number of nodes p, edge covariances $\Sigma_{ij}^* = 0.20$. Plots of probability of correct signed edge-set recovery plotted versus the ordinary sample size n in panel (a), and versus the rescaled sample size $n/\log p$ in panel (b). Each point corresponds to the average over 100 trials.*
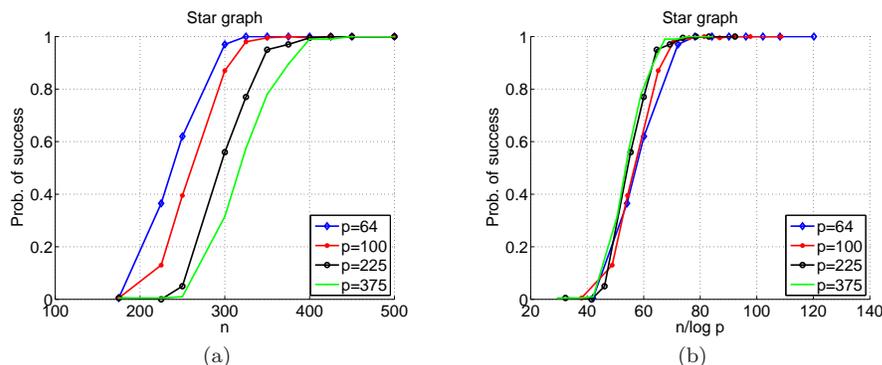
FIG 5. *Simulations for a star graph with varying number of nodes p, fixed maximal degree d = 40, and edge covariances $\Sigma^*_{ij} = 1/16$ for all edges. Plots of probability of correct signed edge-set recovery versus the sample size n in panel (a), and versus the rescaled sample size $n/\log p$ in panel (b). Each point corresponds to the average over $N = 100$ trials.*

node degree is constant $d = 2$, while the edge covariances are set as $\Sigma_{ij} = 0.2$ for all $(i,j) \in E$, so that the quantities $(\kappa_{\Sigma^*}, \kappa_{\Gamma^*}, \alpha)$ remain constant. Each of the curve in panel (a) corresponds to a different graph size p. For each curve, the probability of success starts at zero (for small sample sizes n), but then transitions to one as the sample size is increased. As would be expected, it is more difficult to perform model selection for larger graph sizes, so that (for instance) the curve for $p = 375$ is shifted to the right relative to the curve for $p = 64$. Panel (b) of Figure 4 replots the same data, with the horizontal axis rescaled by $(1/\log p)$. This scaling was chosen because for sub-Gaussian tails, our theory predicts that the sample size should scale logarithmically with p (see equation (66)). Consistent with this prediction, when plotted against the rescaled sample size $n/\log p$, the curves in panel (b) all stack up. Consequently, the ratio $(n/\log p)$ acts as an effective sample size in controlling the success of model selection, consistent with the predictions of Theorem 2 for sub-Gaussian variables.

Figure 5 shows the same types of plots for a star-shaped graph with fixed maximum node degree $d = 40$, and Figure 6 shows the analogous plots for a grid graph with fixed degree $d = 4$. As in the chain case, these plots show the same type of stacking effect in terms of the scaled sample size $n/\log p$, when the degree d and other parameters $((\alpha, \kappa_{\Gamma^*}, \kappa_{\Sigma^*}))$ are held fixed.

5.2. Dependence on the maximum node degree

Panel (a) of Figure 7 plots the probability of correct signed edge-set recovery against the sample size n for star-shaped graphs; each curve corresponds to a different choice of maximum node degree d, allowing us to investigate the dependence of the sample size on this parameter. So as to control these com-
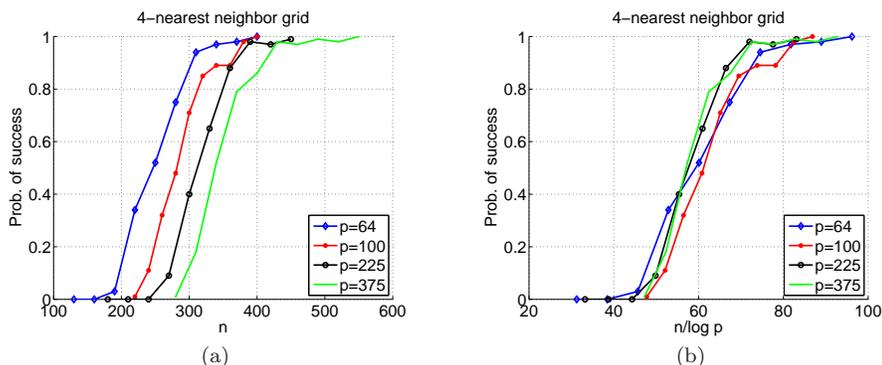
FIG 6. *Simulations for 2-dimensional lattice with 4-nearest-neighbor interaction, edge strength interactions $\Theta^*_{ij} = 0.1$, and a varying number of nodes p. Plots of probability of correct signed edge-set recovery versus the sample size n in panel (a), and versus the rescaled sample size $n/\log p$ in panel (b). Each point corresponds to the average over $N = 100$ trials.*
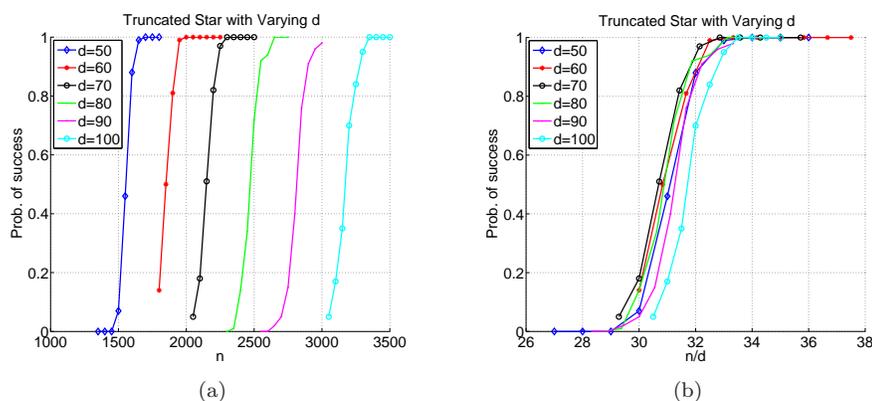

FIG 7. *Simulations for star graphs with fixed number of nodes $p = 200$, varying maximal (hub) degree d, edge covariances $\Sigma^*_{ij} = 2.5/d$. Plots of probability of correct signed edge-set recovery versus the sample size n in panel (a), and versus the rescaled sample size n/d in panel (b).*

parisons, the models are chosen such that quantities other than the maximum node-degree d are fixed: in particular, we fix the number of nodes $p = 200$, and the edge covariance entries are set as $\Sigma^*_{ij} = 2.5/d$ for $(i, j) \in E$ so that the quantities $(\kappa_{\Sigma^*}, \kappa_{\Gamma^*}, \alpha)$ remain constant. The minimum value $\theta_{\min}$ in turn scales as $1/d$. Observe how the plots in panel (a) shift to the right as the maximum node degree d is increased, showing that star-shaped graphs with higher degrees are more difficult. In panel (b) of Figure 7, we plot the same data versus the rescaled sample size n/d. Recall that if all the curves were to stack up under this rescaling, then it means the required sample size n scales linearly with d.
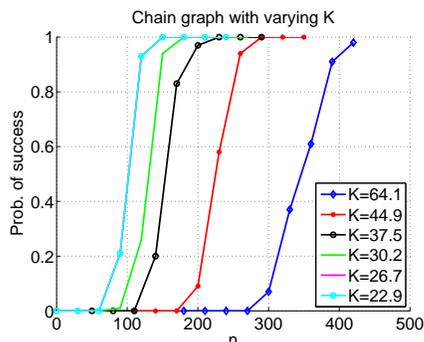
FIG 8. *Simulations for chain graph with fixed number of nodes* $p = 120$*, and varying model complexity* K*. Plot of probability of correct signed edge-set recovery versus the sample size* n*.*

These plots are closer to aligning than the unrescaled plots, but the agreement is not perfect. In particular, observe that the curve $d = 100$ (right-most in panel (a)) remains a bit to the right in panel (b), which suggests that a somewhat more aggressive rescaling—perhaps n/d^γ for some $\gamma \in (1, 2)$—is appropriate.

Note that for $\theta_{\min}$ scaling as $1/d$, the sufficient condition from Theorem 2, as summarized in equation (66), is $n = \Omega(d^2 \log p)$, which appears to be overly conservative based on these data. Thus, it might be possible to tighten our theory under certain regimes.

5.3. Dependence on covariance and Hessian terms

Next, we study the dependence of the sample size required for model selection consistency on the model complexity term K defined in (65), which is a collection of the quantities κ_{Σ^*}, κ_{Γ^*} and α defined by the covariance matrix and Hessian, as well as the minimum value $\theta_{\min}$. Figure 8 plots the probability of correct signed edge-set recovery versus the sample size n for chain graphs. Here each curve corresponds to a different setting of the model complexity factor K, but with a fixed number of nodes $p = 120$, and maximum node-degree $d = 2$. We varied the actor K by varying the value ρ of the edge covariances $\Sigma_{ij} = \rho$, $(i, j) \in E$. Notice how the curves, each of which corresponds to a different model complexity factor, shift rightwards as K is increased so that models with larger values of K require greater number of samples n to achieve the same probability of correct model selection. These rightward-shifts are in qualitative agreement with the prediction of Theorem 1, but we suspect that our analysis is not sharp enough to make accurate quantitative predictions regarding this scaling.

5.4. Convergence rates in elementwise ℓ_∞-norm

Finally, we report some simulation results on the convergence rate in elementwise ℓ_∞-norm. According to Corollary 1, in the case of sub-Gaussian tails, the
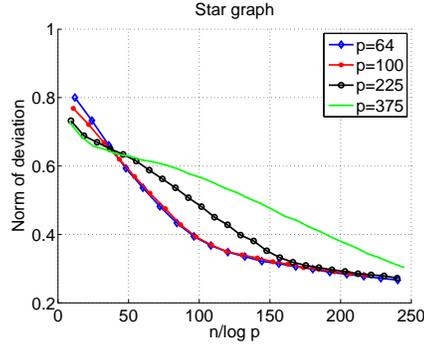
FIG 9. *Simulations for a star graph with varying number of nodes p, maximum node degree $d = \lceil 0.1p \rceil$, edge covariances $\Sigma^*_{ij} = 2.5/d$. Plot of the element-wise ℓ_∞ norm of the concentration matrix estimate error $\|\widehat{\Theta} - \Theta^*\|_\infty$ versus the rescaled sample size $n/\log(p)$.*

elementwise ℓ_∞-norm should decay at the rate $\mathcal{O}(\sqrt{\frac{\log p}{n}})$. Figure 9 shows the behavior of the elementwise ℓ_∞-norm for star-shaped graphs of varying sizes p. The results reported here correspond to the maximum degree $d = \lceil 0.1p \rceil$; we also performed analogous experiments for $d = \mathcal{O}(\log p)$ and $d = \mathcal{O}(1)$, and observed qualitatively similar behavior. The edge correlations were set as $\Sigma^*_{ij} = 2.5/d$ for all $(i,j) \in E$ so that the quantities $(\kappa_{\Sigma^*}, \kappa_{\Gamma^*}, \alpha)$ remain constant. With these settings, each curve in Figure 9 corresponds to a different problem size, and plots the elementwise ℓ_∞-error versus the rescaled sample size $n/\log p$, so that we expect to see curves of the form $f(t) = 1/\sqrt{t}$. The curves show that when the rescaled sample size $(n/\log p)$ is larger than some threshold (roughly 40 in the plots shown), the elementwise ℓ_∞ norm decays at the rate $\sqrt{\frac{\log p}{n}}$, which is consistent with Corollary 1.

6. Discussion

The focus of this paper is the analysis of the high-dimensional scaling of the ℓ_1-regularized log determinant problem (11) as an estimator of the concentration matrix of a random vector. Our main contributions were to derive sufficient conditions for its model selection consistency as well as convergence rates in both elementwise ℓ_∞-norm, as well as Frobenius and spectral norms. Our results allow for a range of tail behavior, ranging from the exponential-type decay provided by Gaussian random vectors (and sub-Gaussian more generally), to polynomial-type decay guaranteed by moment conditions. In the Gaussian case, our results have natural interpretations in terms of Gaussian Markov random fields.

Our main results relate the i.i.d. sample size n to various parameters of the problem required to achieve consistency. In addition to the dependence on matrix size p, number of edges s and graph degree d, our analysis also illustrates the role of other quantities, related to the structure of the covariance matrix Σ^*

and the Hessian of the objective function, that have an influence on consistency rates. Our main assumption is an irrepresentability or mutual incoherence condition, similar to that required for model selection consistency of the Lasso, but involving the Hessian of the log-determinant objective function (11), evaluated at the true model. Such an irrepresentability condition is typical for obtaining model selection consistency, but is not necessary for bounds on Frobenius and spectral norms [27]. When the distribution of X is multivariate Gaussian, this Hessian is the Fisher information matrix of the model, and thus can be viewed as an edge-based counterpart to the usual node-based covariance matrix. We report some examples where irrepresentability condition for the Lasso hold and the log-determinant condition fails, but we do not know in general if one requirement dominates the other. In addition to these theoretical results, we provided a number of simulation studies showing how the sample size required for consistency scales with problem size, node degrees, and the other complexity parameters identified in our analysis.

There are various interesting questions and possible extensions to this paper. First, in the current paper, we have only derived sufficient conditions for model selection consistency. As in past work on the Lasso [29], it would also be interesting to derive a *converse result*—namely, to prove that if the sample size n is smaller than some function of (p, d, s) and other complexity parameters, then regardless of the choice of regularization constant, the log-determinant method fails to recover the correct graph structure. Second, while this paper studies the problem of estimating a fixed graph or concentration matrix, a natural extension would allow the graph to vary over time, a problem setting which includes the case where the observations are dependent. For instance, Zhou et al. [33] study the estimation of the covariance matrix of a Gaussian distribution in a time-varying setting, and it would be interesting to extend results of this paper to this more general setting.

Acknowledgements

Appendix A: Proof of Lemma 3

In this appendix, we show that the regularized log-determinant program (11) has a unique solution whenever $\lambda_n > 0$, and the diagonal elements of the sample covariance $\widehat{\Sigma}^n$ are strictly positive. By the strict convexity of the log-determinant barrier [3], if the minimum is attained, then it is unique, so that it remains to show that the minimum is achieved. If $\lambda_n > 0$, then by Lagrangian duality, the

problem can be written in an equivalent constrained form:

$$\min_{\Theta \in \mathcal{S}_{++}^p, \|\Theta\|_{1,\text{off}} \leq C(\lambda_n)} \left\{ \langle\!\langle \Theta, \, \widehat{\Sigma}^n \rangle\!\rangle - \log \det(\Theta) \right\} \tag{67}$$

for some $C(\lambda_n) < +\infty$. Since the off-diagonal elements remain bounded within the ℓ_1-ball, the only possible issue is the behavior of the objective function for sequences with possibly unbounded diagonal entries. Since any Θ in the constraint set is positive-definite, its diagonal entries are positive. Further, by Hadamard's inequality for positive definite matrices [14], we have $\log \det \Theta \leq \sum_{i=1}^p \log \Theta_{ii}$, so that

$$\sum_{i=1}^p \Theta_{ii} \widehat{\Sigma}_{ii}^n - \log \det \Theta \quad \geq \quad \sum_{i=1}^p \left\{ \Theta_{ii} \widehat{\Sigma}_{ii}^n - \log \Theta_{ii} \right\}.$$

As long as $\widehat{\Sigma}_{ii}^n > 0$ for each $i = 1, \ldots, p$, this function is coercive, meaning that it diverges to infinity for any sequence $\|(\Theta_{11}^t, \ldots, \Theta_{pp}^t)\|_2 \to +\infty$. Consequently, the minimum is attained, and as argued above, is also unique.

Returning to the penalized form (11), by standard optimality conditions for convex programs, a matrix $\widehat{\Theta} \in \mathcal{S}_{++}^p$ is optimal for (11) if and only the zero matrix belongs to the sub-differential of the objective, or equivalently if and only if there exists a matrix $\widehat{Z}$ in the sub-differential of the off-diagonal norm $\| \cdot \|_{1,\text{off}}$ evaluated at $\widehat{\Theta}$ such that

$$\widehat{\Sigma} - \widehat{\Theta}^{-1} + \lambda \widehat{Z} = 0,$$

as claimed.

Appendix B: Proof of Lemma 5

We write the remainder in the form

$$R(\Delta) \quad = \quad (\Theta^* + \Delta)^{-1} - \Theta^{*-1} + \Theta^{*-1} \Delta \Theta^{*-1}.$$

By sub-multiplicativity of the $\| \cdot \|_\infty$ matrix norm, for any two $p \times p$ matrices A, B, we have $\|A B\|_\infty \leq \|A\|_\infty \|B\|_\infty$, so that

$$\begin{aligned} \|\Theta^{*-1} \Delta\|_\infty &\leq \|\Theta^{*-1}\|_\infty \|\Delta\|_\infty \\ &\leq \kappa_{\Sigma^*} \, d \|\Delta\|_\infty \ < \ 1/3, \end{aligned} \tag{68}$$

where we have used the definition of κ_{Σ^*}, the fact that Δ has at most d non-zeros per row/column, and our assumption $\|\Delta\|_\infty < 1/(3\kappa_{\Sigma^*} p)$. Consequently,

we have the convergent matrix expansion

$$
\begin{aligned}
\left(\Theta^* + \Delta\right)^{-1} &= \left(\Theta^*\left(I + \Theta^{*-1}\Delta\right)\right)^{-1} \\
&= \left(I + \Theta^{*-1}\Delta\right)^{-1}\left(\Theta^*\right)^{-1} \\
&= \sum_{k=0}^{\infty}(-1)^k\left(\Theta^{*-1}\Delta\right)^k\left(\Theta^*\right)^{-1} \\
&= \Theta^{*-1} - \Theta^{*-1}\Delta\Theta^{*-1} + \sum_{k=2}^{\infty}(-1)^k\left(\Theta^{*-1}\Delta\right)^k\left(\Theta^*\right)^{-1} \\
&= \Theta^{*-1} - \Theta^{*-1}\Delta\Theta^{*-1} + \Theta^{*-1}\Delta\Theta^{*-1}\Delta J\Theta^{*-1},
\end{aligned}
$$

where $J = \sum_{k=0}^{\infty}(-1)^k\left(\Theta^{*-1}\Delta\right)^k$.

We now prove the bound (57) on the remainder as follows. Let e_i denote the unit vector with 1 in position i and zeroes elsewhere. From equation (56), we have

$$
\begin{aligned}
\|R(\Delta)\|_{\infty} &= \max_{i,j}|e_i^T\Theta^{*-1}\Delta\,\Theta^{*-1}\Delta J\Theta^{*-1}e_j| \\
&\leq \max_i\|e_i^T\Theta^{*-1}\Delta\|_{\infty}\max_j\|\Theta^{*-1}\Delta J\Theta^{*-1}e_j\|_1,
\end{aligned}
$$

which follows from the fact that for any vectors $a, b \in \mathbb{R}^p$, $|a^T b| \leq \|a\|_{\infty}\|b\|_1$. This in turn can be simplified as,

$$
\|R(\Delta)\|_{\infty} \leq \max_i\|e_i^T\Theta^{*-1}\|_1\,\|\Delta\|_{\infty}\max_j\|\Theta^{*-1}\Delta J\Theta^{*-1}e_j\|_1
$$

since for any vector $u \in \mathbb{R}^p$, $\|u^T\Delta\|_{\infty} \leq \|u\|_1\|\Delta\|_{\infty}$, where $\|\Delta\|_{\infty}$ is the elementwise ℓ_{∞}-norm. Continuing on, we have

$$
\|R(\Delta)\|_{\infty} \leq \|\!|\Theta^{*-1}|\!\|_{\infty}\,\|\Delta\|_{\infty}\|\,\|\!|\Theta^{*-1}\Delta J\Theta^{*-1}|\!\|_1,
$$

where $\|\!|A|\!\|_1 := \max_{\|x\|_1=1}\|Ax\|_1$ is the ℓ_1-operator norm. Since $\|\!|A|\!\|_1 = \|\!|A^T|\!\|_{\infty}$, we have

$$
\begin{aligned}
\|R(\Delta)\|_{\infty} &\leq \|\Delta\|_{\infty}\|\!|\Theta^{*-1}|\!\|_{\infty}\,\|\!|\Theta^{*-1}J^T\Delta\Theta^{*-1}|\!\|_{\infty} \\
&\leq \|\Delta\|_{\infty}\,\kappa_{\Sigma^*}\|\!|\Theta^{*-1}|\!\|_{\infty}^2\|\!|J^T|\!\|_{\infty}\|\Delta\|_{\infty} \quad\quad (69)
\end{aligned}
$$

Recall that $J = \sum_{k=0}^{\infty}(-1)^k\left(\Theta^{*-1}\Delta\right)^k$. By sub-multiplicativity of $\|\!|\cdot|\!\|_{\infty}$ matrix norm, we have

$$
\|\!|J^T|\!\|_{\infty} \leq \sum_{k=0}^{\infty}\|\!|\Delta\Theta^{*-1}|\!\|_{\infty}^k \leq \frac{1}{1 - \|\!|\Theta^{*-1}|\!\|_{\infty}\|\Delta\|_{\infty}} \leq \frac{3}{2},
$$

since $\|\!|\Theta^{*-1}|\!\|_{\infty}\|\Delta\|_{\infty} < 1/3$ from equation (68). Substituting this in (69), we obtain

$$
\begin{aligned}
\|R(\Delta)\|_{\infty} &\leq \frac{3}{2}\|\Delta\|_{\infty}\,\kappa_{\Sigma^*}\|\!|\Theta^{*-1}|\!\|_{\infty}^2\|\Delta\|_{\infty} \\
&\leq \frac{3}{2}d\|\Delta\|_{\infty}^2\,\kappa_{\Sigma^*}^3,
\end{aligned}
$$

where the final line follows since $\|\Delta\|_\infty \le d\|\Delta\|_\infty$, and since Δ has at most d non-zeroes per row/column.

Appendix C: Proof of Lemma 6

By following the same argument as Lemma 3 in Appendix A, we conclude that the restricted problem (47) has a unique optimum $\widetilde{\Theta}$. If we take partial derivatives of the Lagrangian of the restricted problem (47) with respect to the unconstrained elements Θ_S, these partial derivatives must vanish at the optimum, meaning that we have the zero-gradient condition

$$G(\Theta_S) \;=\; -[\Theta^{-1}]_S + \widehat{\Sigma}_S + \lambda_n \widetilde{Z}_S \;=\; 0. \tag{70}$$

To be clear, Θ is the $p \times p$ matrix with entries in S equal to Θ_S and entries in S^c equal to zero. Since this zero-gradient condition is necessary and sufficient for an optimum of the Lagrangian problem, it has a unique solution (namely, $\widetilde{\Theta}_S$).

Our goal is to bound the deviation of this solution from Θ_S^*, or equivalently to bound the deviation $\Delta = \widetilde{\Theta} - \Theta^*$. Our strategy is to show the existence of a solution Δ to the zero-gradient condition (70) that is contained inside the ball $\mathbb{B}(r)$ defined in equation (60). By uniqueness of the optimal solution, we can thus conclude that $\widetilde{\Theta} - \Theta^*$ belongs this ball. In terms of the vector $\overline{\Delta}_S = \overline{\widetilde{\Theta}}_S - \overline{\Theta^*}_S$, let us define a map $F : \mathbb{R}^{|S|} \to \mathbb{R}^{|S|}$ via

$$F(\overline{\Delta}_S) \;:=\; -(\Gamma_{SS}^*)^{-1}(\overline{G}(\Theta_S^* + \Delta_S)) + \overline{\Delta}_S, \tag{71}$$

where $\overline{G}$ denotes the vectorized form of G. Note that by construction, $F(\overline{\Delta}_S) = \overline{\Delta}_S$ holds if and only if $G(\Theta_S^* + \Delta_S) = G(\widetilde{\Theta}_S) = 0$.

We now claim that $F(\mathbb{B}(r)) \subseteq \mathbb{B}(r)$. Since F is continuous and $\mathbb{B}(r)$ is convex and compact, this inclusion implies, by Brouwer's fixed point theorem [23], that there exists some fixed point $\overline{\Delta}_S \in \mathbb{B}(r)$. By uniqueness of the zero gradient condition (and hence fixed points of F), we can thereby conclude that $\|\widetilde{\Theta}_S - \Theta_S^*\|_\infty \le r$.

Let $\Delta \in \mathbb{R}^{p \times p}$ denote the zero-padded matrix, equal to Δ_S on S and zero on S^c. By definition, we have

$$
\begin{aligned}
G(\Theta_S^* + \Delta_S) \;&=\; -[(\Theta^* + \Delta)^{-1}]_S + \widehat{\Sigma}_S + \lambda_n \widetilde{Z}_S \\
&=\; \big[-[(\Theta^* + \Delta)^{-1}]_S + [\Theta^{*-1}]_S\big] + \big[\widehat{\Sigma}_S - [\Theta^{*-1}]_S\big] + \lambda_n \widetilde{Z}_S \\
&=\; \big[-[(\Theta^* + \Delta)^{-1}]_S + [\Theta^{*-1}]_S\big] + W_S + \lambda_n \widetilde{Z}_S, \tag{72}
\end{aligned}
$$

where we have used the definition $W = \widehat{\Sigma} - \Sigma^*$.

For any $\Delta_S \in \mathbb{B}(r)$, we have

$$
\begin{aligned}
\|\Theta^{*-1}\Delta\|_\infty \;&\le\; \|\Theta^{*-1}\|_\infty \|\Delta\|_\infty \\
&\le\; \kappa_{\Sigma^*}\, d\|\Delta\|_\infty, \tag{73}
\end{aligned}
$$

where $\|\Delta\|_\infty$ denotes the elementwise ℓ_∞-norm (as opposed to the ℓ_∞-operator norm $\|\|\Delta\|\|_\infty$), and the inequality follows since Δ has at most d non-zero entries per row/column.

By the definition (60) of the radius r, and the assumed upper bound (58), we have $\|\Delta\|_\infty \leq r \leq \frac{1}{3\kappa_{\Sigma^*}d}$, so that the results of Lemma 5 apply. By using the definition (50) of the remainder, taking the vectorized form of the expansion (56), and restricting to entries in S, we obtain the expansion

$$\text{vec}\left((\Theta^* + \Delta)^{-1} - \Theta^{*-1}\right)_S + \Gamma^*_{SS}\overline{\Delta}_S \;=\; \text{vec}\left((\Theta^{*-1}\Delta)^2 J\Theta^{*-1}\right)_S. \quad (74)$$

Using this expansion (74) combined with the expression (72) for G, we have

$$\begin{aligned}
F(\overline{\Delta}_S) &= -\left(\Gamma^*_{SS}\right)^{-1}\overline{G}(\Theta^*_S + \Delta_S) + \overline{\Delta}_S \\
&= \left(\Gamma^*_{SS}\right)^{-1}\text{vec}\left\{\left[(\Theta^* + \Delta)^{-1} - \Theta^{*-1}\right]_S - W_S - \lambda_n\widetilde{Z}_S\right\} + \overline{\Delta}_S \\
&= \underbrace{\left(\Gamma^*_{SS}\right)^{-1}\text{vec}\left[(\Theta^{*-1}\Delta)^2 J\Theta^{*-1}\right]_S}_{T_1} - \underbrace{\left(\Gamma^*_{SS}\right)^{-1}\left(\overline{W}_S + \lambda_n\overline{\widetilde{Z}}_S\right)}_{T_2}.
\end{aligned}$$

The second term is easy to deal with: using the definition $\kappa_{\Gamma^*} = \|\|(\Gamma^*_{SS})^{-1}\|\|_\infty$, we have $\|T_2\|_\infty \leq \kappa_{\Gamma^*}\left(\|W\|_\infty + \lambda_n\right) \;=\; r/2$. It now remains to show that $\|T_1\|_\infty \leq r/2$. We have

$$\begin{aligned}
\|T_1\|_\infty &\leq \kappa_{\Gamma^*}\left\|\text{vec}\left[(\Theta^{*-1}\Delta)^2 J\Theta^{*-1}\right]_S\right\|_\infty \\
&\leq \kappa_{\Gamma^*}\|R(\Delta)\|_\infty,
\end{aligned}$$

where we used the expanded form (56) of the remainder. Applying the bound (57) from Lemma 5, we obtain

$$\|T_1\|_\infty \;\leq\; \frac{3}{2}d\kappa^3_{\Sigma^*}\kappa_{\Gamma^*}\|\Delta\|^2_\infty \;\leq\; \frac{3}{2}d\kappa^3_{\Sigma^*}\kappa_{\Gamma^*}\,r^2.$$

Since $r \leq \frac{1}{3\kappa^3_{\Sigma^*}\kappa_{\Gamma^*}d}$ by assumption (58), we conclude that

$$\|T_1\|_\infty \;\leq\; \frac{3}{2}d\kappa^3_{\Sigma^*}\kappa_{\Gamma^*}\frac{1}{3\kappa^3_{\Sigma^*}\kappa_{\Gamma^*}d}r \;=\; r/2,$$

thereby establishing the claim.

Appendix D: Proof of Lemma 1

For each pair (i, j) and $\nu > 0$, define the event

$$\mathbb{A}_{ij}(\nu) \;:=\; \left\{\left|\frac{1}{n}\sum_{k=1}^n X_i^{(k)}X_j^{(k)} - \Sigma^*_{ij}\right| > \nu\right\}.$$

As the sub-Gaussian assumption is imposed on the variables $\{X_i^{(k)}\}$ directly, as in Lemma A.3 of Bickel and Levina [2], our proof proceeds by first decoupling the

products $X_i^{(k)} X_j^{(k)}$. For each pair (i,j), we define $\rho_{ij}^* = \Sigma_{ij}^* / \sqrt{\Sigma_{ii}^* \Sigma_{jj}^*}$, and the rescaled random variables $\overline{X}_i^{(k)} := X_{ij}^{(k)} / \sqrt{\Sigma_{ii}^*}$. Noting that the strict positive definiteness of Σ^* implies that $|\rho_{ij}^*| < 1$, we can also define the auxiliary random variables

$$U_{ij}^{(k)} := \overline{X}_i^{(k)} + \overline{X}_j^{(k)} \quad \text{and} \quad V_{ij}^{(k)} := \overline{X}_i^{(k)} - \overline{X}_j^{(k)}. \tag{75}$$

With this notation, we then claim:

Lemma 9. *Suppose that each $\overline{X}_i^{(k)}$ is sub-Gaussian with parameter σ. Then for each node pair (i,j), the following properties hold:*

(a) *For all $k = 1, \ldots, n$, the random variables $U_{ij}^{(k)}$ and $V_{ij}^{(k)}$ are sub-Gaussian with parameters 2σ.*

(b) *For all $\nu > 0$, the probability $\mathbb{P}[\mathbb{A}_{ij}(\nu)]$ is upper bounded by*

$$\mathbb{P}\left[\left|\sum_{k=1}^n (U_{ij}^{(k)})^2 - 2(1 + \rho_{ij}^*)\right| > \frac{2n\nu}{\sqrt{\Sigma_{ii}^* \Sigma_{jj}^*}}\right]$$

$$+ \mathbb{P}\left[\left|\sum_{k=1}^n (V_{ij}^{(k)})^2 - 2(1 - \rho_{ij}^*)\right| > \frac{2n\nu}{\sqrt{\Sigma_{ii}^* \Sigma_{jj}^*}}\right].$$

Proof. (a) For any $r \in \mathbb{R}$, we have

$$\begin{aligned}
\mathbb{E}[\exp(r U_{ij}^{(k)})] &= \mathbb{E}\left[\exp\left(r \overline{X}_i^{(k)}\right) \exp\left(r \overline{X}_j^{(k)}\right)\right] \\
&\leq \mathbb{E}\left[\exp\left(2r \overline{X}_i^{(k)}\right)\right]^{1/2} \left[\exp\left(2r \overline{X}_j^{(k)}\right)\right]^{1/2},
\end{aligned}$$

where we have used the Cauchy-Schwarz inequality. Since the variables $\overline{X}_i^{(k)}$ and $\overline{X}_j^{(k)}$ are sub-Gaussian with parameter σ, we have

$$\mathbb{E}\left[\exp\left(2r \overline{X}_i^{(k)}\right)\right]^{1/2} \mathbb{E}\left[\exp\left(2r \overline{X}_j^{(k)}\right)\right]^{1/2} \leq \exp\left(\sigma^2 \frac{r^2}{2}\right) \exp\left(\sigma^2 \frac{r^2}{2}\right),$$

so that $U_{ij}^{(k)}$ is sub-Gaussian with parameter 2σ as claimed.

(b) By straightforward algebra, we have the decomposition

$$\begin{aligned}
\sum_{k=1}^n (\overline{X}_i^{(k)} \overline{X}_j^{(k)} - \rho_{ij}^*) &= \left\{\frac{1}{4}\sum_{i=1}^n \left\{(\overline{X}_i^{(k)} + \overline{X}_j^{(k)})^2 - 2(1 + \rho_{st}^*)\right\}\right\} \\
&\quad - \left\{\frac{1}{4}\sum_{i=1}^n \left\{(X_s^{*(k)} - X_t^{*(k)})^2 - 2(1 - \rho_{st}^*)\right\}\right\}.
\end{aligned}$$

By union bound, we obtain that $\mathbb{P}[\mathbb{A}_{ij}(\nu)]$ is upper bounded by

$$\mathbb{P}\left[\left|\sum_{k=1}^n (U_{ij}^{(k)})^2 - 2(1 + \rho_{ij}^*)\right| \geq \frac{4n\nu}{2\sqrt{\Sigma_{ii}^* \Sigma_{jj}^*}}\right]$$

$$+ \mathbb{P}\left[\left|\sum_{k=1}^n (V_{ij}^{(k)})^2 - 2(1 - \rho_{ij}^*)\right| \geq \frac{4n\nu}{2\sqrt{\Sigma_{ii}^* \Sigma_{jj}^*}}\right], \tag{76}$$

which completes the proof of Lemma 9(b). $\qquad\square$

To complete the proof of Lemma 1, it remains to upper bound the tail probabilities

$$\mathbb{P}\left[\left|\sum_{k=1}^{n}(U_{ij}^{(k)})^2 - 2\left(1 + \rho_{ij}^*\right)\right| \geq \frac{4n\nu}{2\sqrt{\Sigma_{ii}^*\Sigma_{jj}^*}}\right],$$

and

$$\mathbb{P}\left[\left|\sum_{k=1}^{n}(V_{ij}^{(k)})^2 - 2\left(1 - \rho_{ij}^*\right)\right| \geq \frac{4n\nu}{2\sqrt{\Sigma_{ii}^*\Sigma_{jj}^*}}\right].$$

For all $k \in \{1,\ldots,n\}$ and node-pairs $(i,j) \in V \times V$, define the random variables $Z_{k;ij}$ as follows:

$$Z_{k;ij} \quad := \quad (U_{ij}^{(k)})^2 - 2\left(1 + \rho_{ij}^*\right).$$

If we can obtain a bound $B > 0$ such that

$$\sup_{m \geq 2}\left[\frac{\mathbb{E}(|Z_{k;ij}|^m)}{m!}\right]^{1/m} \quad \leq \quad B/2,$$

it then follows from Bernstein's inequality based on moment conditions that:

$$\mathbb{P}\left[\left|\sum_{k=1}^{n}|Z_{k;ij}|\right| \geq nt\right] \leq 2\exp\left(-\frac{nt^2}{2B^2 + 2tB}\right). \tag{77}$$

Furthermore for $t \leq B$,

$$\mathbb{P}\left[\left|\sum_{k=1}^{n}|Z_{k;ij}|\right| \geq nt\right] \leq 2\exp\left(-\frac{nt^2}{4B^2}\right). \tag{78}$$

Using the bound $(a + b)^m \leq 2^m(a^m + b^m)$ we obtain the inequality:

$$\mathbb{E}(|Z_{k;ij}|^m) \quad \leq \quad 2^m\left(\mathbb{E}(|U_{ij}^{(k)}|^{2m}) + (2(1 + \rho_{ij}^*))^m\right). \tag{79}$$

Recalling that $U_{ij}^{(k)}$ is sub-Gaussian with parameter 2σ, from Lemma 1.4 of Buldygin and Kozachenko [6] regarding the moments of sub-Gaussian variates, we have $\mathbb{E}[|U_{ij}^{(k)}|^{2m}] \leq 2(2m/e)^m(2\sigma)^{2m}$. Making note of the inequality $m! \geq (m/e)^m$, it follows that $\mathbb{E}[|U_{ij}^{(k)}|^{2m}]/m! \leq 2^{3m+1}\sigma^{2m}$. Combined with equation (79), we obtain

$$\left[\frac{\mathbb{E}(|Z_{k;ij}|^m)}{m!}\right]^{1/m} \quad \leq \quad 2^{1/m}\left((2^{4m+1}\sigma^{2m})^{1/m} + \frac{4(1 + \rho_{ij}^*)}{(m!)^{1/m}}\right)$$

$$\leq \quad 2^{1/m}\left(2^{1/m}\,16\,\sigma^2 + \frac{4(1 + \rho_{ij}^*)}{(m!)^{1/m}}\right),$$

where we have used the inequality $(x + y)^{1/m} \leq 2^{1/m}(x^{1/m} + y^{1/m})$, valid for any integer $m \in \mathbb{N}$ and real numbers $x, y > 0$. Since the bound is a decreasing function of m, it follows that

$$
\sup_{m \geq 2} \left[\frac{\mathbb{E}(|Z_{k;ij}|^m)}{m!} \right]^{1/m} \quad \leq \quad 2^{1/2} \left(2^{1/2} \, 16 \, \sigma^2 + \frac{4(1 + \rho_{ij}^*)}{(2)^{1/2}} \right)
$$

$$
\leq \quad 32\sigma^2 + 8 = 8(1 + 4\sigma^2),
$$

where we have used the fact that $|\rho_{ij}^*| \leq 1$. Applying Bernstein's inequality (78) with $t = \frac{2\nu}{\max_i \Sigma_{ii}^*}$ and $B = 8(1 + 4\sigma^2)$, noting that $\left(\frac{2\nu}{\max_i \Sigma_{ii}^*} \right) \leq \left(\frac{2\nu}{\sqrt{\Sigma_{ii}^* \Sigma_{jj}^*}} \right)$, for $\nu \leq 8(\max_i \Sigma_{ii}^*)(1 + 4\sigma^2)$,

$$
\mathbb{P}\left[\left| \sum_{k=1}^n (U_{ij}^{(k)})^2 - 2\,(1 + \rho_{ij}^*) \right| \geq \frac{4n\nu}{2\sqrt{\Sigma_{ii}^* \Sigma_{jj}^*}} \right] \leq 2\exp\left\{ -\frac{2n\nu^2}{\max_i(\Sigma_{ii}^*)^2 128(1 + 4\sigma^2)^2} \right\}.
$$

A similar argument yields the same tail bound for the deviation involving $V_{ij}^{(k)}$. Consequently, using Lemma 9(b), we conclude that

$$
\mathbb{P}[\mathbb{A}_{ij}(\nu)] \quad \leq \quad 4\exp\left\{ -\frac{n\nu^2}{\max_i(\Sigma_{ii}^*)^2 \, 128\,(1 + 4\sigma^2)^2} \right\},
$$

valid for $\nu \leq 8(\max_i \Sigma_{ii}^*)\,(1 + 4\sigma^2)$, as required.

Appendix E: Proof of Lemma 2

Define the random variables $W_{ij}^{(k)} = X_i^{(k)} X_j^{(k)} - \Sigma_{ij}^*$, and note that they have mean zero. By applying the Chebyshev inequality, we obtain

$$
\mathbb{P}\left[\left| \sum_{k=1}^n W_{ij}^{(k)} \right| > n\,\nu \right] \quad = \quad \mathbb{P}\left[\left(\sum_{k=1}^n W_{ij}^{(k)} \right)^{2m} > (n\,\nu)^{2m} \right]
$$

$$
\leq \quad \frac{\mathbb{E}\left[\left(\sum_{k=1}^n W_{ij}^{(k)} \right)^{2m} \right]}{n^{2m}\,\nu^{2m}}. \tag{80}
$$

We now apply Rosenthal's inequality [26] to obtain that there exists[2] a constant C_m, depending only on m, such that

$$
\mathbb{E}\left[\left(\sum_{k=1}^n W_{ij}^{(k)} \right)^{2m} \right] \quad \leq \quad C_m \max\left(\sum_{k=1}^n \mathbb{E}[(W_{ij}^{(k)})^{2m}], \left(\sum_{k=1}^n \mathbb{E}[(W_{ij}^{(k)})^2] \right)^m \right)
$$

$$
\leq \quad C_m \left(\sum_{k=1}^n \mathbb{E}[(W_{ij}^{(k)})^{2m}] + \left(\sum_{k=1}^n \mathbb{E}[(W_{ij}^{(k)})^2] \right)^m \right). \tag{81}
$$

---

[2]For precise values of C_m, see Rosenthal [26].

Turning to each individual expectation, we have

$$
\begin{aligned}
\mathbb{E}[\big(W_{ij}^{(k)}\big)^{2m}] &\leq \quad \mathbb{E}[(X_i^{(k)} X_j^{(k)} - \Sigma_{ij}^*)^{2m}] \\
&\stackrel{(i)}{\leq} \quad 2^{2m}\big\{\mathbb{E}[(X_i^{(k)} X_j^{(k)})^{2m}] + [\Sigma_{ij}^*]^{2m}\big\} \\
&\stackrel{(ii)}{\leq} \quad 2^{2m}\big\{\sqrt{\mathbb{E}[(X_i^{(k)})^{4m}]\mathbb{E}[(X_j^{(k)})^{4m}]} + [\Sigma_{ij}^*]^{2m}\big\} \\
&\stackrel{(iii)}{\leq} \quad 2^{2m}(K_m[\Sigma_{ii}^*\Sigma_{jj}^*]^m + [\Sigma_{ij}^*]^{2m}),
\end{aligned}
$$

where inequality (i) follows since $(a+b)^{2m} \leq 2^{2m}(a^{2m} + b^{2m})$; inequality (ii) follows from the Cauchy-Schwartz inequality; and inequality (iii) follows from the assumed moment bound on $\mathbb{E}[(X_i^{(k)})^{4m}]$. Therefore for $m = 1$, we have the have the bound.

$$
\mathbb{E}[\big(W_{ij}^{(k)}\big)^{2}] \quad \leq \quad 4(\Sigma_{ii}^*\Sigma_{jj}^* + [\Sigma_{ij}^*]^2),
$$

and hence

$$
\left(\sum_{k=1}^{n} \mathbb{E}[(W_{ij}^{(k)})^2]\right)^m \quad \leq \quad 2^{2m} n^m ([\Sigma_{ii}^*\Sigma_{jj}^*]^m + [\Sigma_{ij}^*]^{2m}).
$$

Combined with the earlier bound (81) and noting that $n \leq n^m$, we obtain

$$
\mathbb{E}\left[\left(\sum_{k=1}^{n} W_{ij}^{(k)}\right)^{2m}\right] \quad \leq \quad 2^{2m} C_m n^m \big((K_m + 1)[\Sigma_{ii}^*\Sigma_{jj}^*]^m + [\Sigma_{ij}^*]^{2m}\big),
$$

using the Cauchy-Schwartz inequality. Substituting back into the Chebyshev bound (80) yields the tail bound

$$
\begin{aligned}
\mathbb{P}\left[\left|\sum_{k=1}^{n} W_{ij}^{(k)}\right| > n\,\nu\right] &\leq \quad \frac{\left[n^m 2^{2m} C_m ((K_m + 1)[\Sigma_{ii}^*\Sigma_{jj}^*]^m + [\Sigma_{ij}^*]^{2m})\right]}{n^{2m}\,\nu^{2m}} \\
&= \quad \frac{\left[2^{2m} C_m ((K_m + 1)[\Sigma_{ii}^*\Sigma_{jj}^*]^m + [\Sigma_{ij}^*]^{2m})\right]}{n^m \nu^{2m}},
\end{aligned}
$$

which establishes the claim.

References

[1] P. J. BICKEL AND E. LEVINA. Covariance regularization by thresholding. *Ann. Statist.*, 36(6):2577–2604, 2008. MR2485008

[2] P. J. BICKEL AND E. LEVINA. Regularized estimation of large covariance matrices. *Ann. Statist.*, 36(1):199–227, 2008. MR2387969

[3] S. BOYD AND L. VANDENBERGHE. *Convex optimization.* Cambridge University Press, Cambridge, UK, 2004. MR2061575

[4] L. M. BREGMAN. The relaxation method for finding the common point of convex sets and its application to the solution of problems in convex programming. *USSR Computational Mathematics and Mathematical Physics*, 7:191–204, 1967. MR0215617

[5] L. D. BROWN. *Fundamentals of statistical exponential families.* Institute of Mathematical Statistics, Hayward, CA, 1986. MR0882001

[6] V. V. BULDYGIN AND Y. V. KOZACHENKO. *Metric characterization of random variables and random processes.* American Mathematical Society, Providence, RI, 2000. MR1743716

[7] T. T. CAI, C.-H. ZHANG, AND H. H. ZHOU. Optimal rates of convergence for covariance matrix estimation. *Annals of Statistics*, 2010. To appear. MR2676885

[8] Y. CENSOR AND S. A. ZENIOS. *Parallel Optimization: Theory, Algorithms, and Applications.* Numerical Mathematics and Scientific Computation. Oxford University Press, 1988. MR1486040

[9] A. D'ASPRÉMONT, O. BANERJEE, AND L. EL GHAOUI. First-order methods for sparse covariance selection. *SIAM J. Matrix Anal. Appl.*, 30(1):56–66, 2008. MR2399568

[10] N. EL KAROUI. Operator norm consistent estimation of large dimensional sparse covariance matrices. *Ann. Statist.*, To appear, 2008. MR2485011

[11] J. FRIEDMAN, T. HASTIE, AND R. TIBSHIRANI. Sparse inverse covariance estimation with the graphical Lasso. *Biostat.*, 9(3):432–441, 2007.

[12] R. FURRER AND T. BENGTSSON. Estimation of high-dimensional prior and posterior covariance matrices in kalman filter variants. *J. Multivar. Anal.*, 98(2):227–255, 2007. MR2301751

[13] C. GIRAUD. Estimation of gaussian graph by model selection. *Electronic Journal of Statistics*, 2:542–563, 2008. MR2417393

[14] R. A. HORN AND C. R. JOHNSON. *Matrix Analysis.* Cambridge University Press, Cambridge, 1985. MR0832183

[15] J. Z. HUANG, N. LIU, M. POURAHMADI, AND L. LIU. Covariance matrix selection and estimation via penalised normal likelihood. *Biometrika*, 93(1):85–98, 2006. MR2277742

[16] I. M. JOHNSTONE. On the distribution of the largest eigenvalue in principal components analysis. *Ann. Statist.*, 29(2):295–327, 2001. MR1863961

[17] I. M. JOHNSTONE AND A. Y. LU. Sparse principal components analysis. *Unpublished Manuscript*, 2004.

[18] C. LAM AND J. FAN. Sparsistency and rates of convergence in large covariance matrix estimation. *Annals of Statistics*, 37:4254–4278, 2009. MR2572459

[19] O. LEDOIT AND M. WOLF. A well-conditioned estimator for large-dimensional covariance matrices. *J. Multivar. Anal.*, 88:365–411, 2003. MR2026339

[20] M. LEDOUX. *The Concentration of Measure Phenomenon.* Mathematical Surveys and Monographs. American Mathematical Society, Providence, RI, 2001. MR1849347

[21] N. MEINSHAUSEN. A note on the Lasso for graphical Gaussian model selection. *Statistics and Probability Letters*, 78(7): 880–884, 2008. MR2398362

[22] N. MEINSHAUSEN AND P. BÜHLMANN. High-dimensional graphs and variable selection with the Lasso. *Ann. Statist.*, 34(3):1436–1462, 2006.

[23] J. M. ORTEGA AND W. G. RHEINBOLDT. *Iterative Solution of Nonlinear Equations in Several Variables.* Academic Press, NY, 1970. MR0273810

[24] V. V. PETROV. *Limit Theorems Of Probability Theory: Sequences Of Independent Random Variables.* Oxford University Press, Oxford, UK, 1995. MR1353441

[25] P. RAVIKUMAR, M. J. WAINWRIGHT, G. RASKUTTI, AND B. YU. High-dimensional covariance estimation: Convergence rates of ℓ_1-regularized log-determinant divergence. Technical report, Department of Statistics, UC Berkeley, September 2008.

[26] H. P. ROSENTHAL. On the subspaces of l^p $(p > 2)$ spanned by sequences of independent random variables. *Israel J. Math*, 8:1546–1570, 1970. MR0271721

[27] A. J. ROTHMAN, P. J. BICKEL, E. LEVINA, AND J. ZHU. Sparse permutation invariant covariance estimation. *Electron. J. Statist.*, 2:494–515, 2008. MR2417391

[28] J. A. TROPP. Just relax: Convex programming methods for identifying sparse signals. *IEEE Trans. Info. Theory*, 51(3): 1030–1051, 2006. MR2238069

[29] M. J. WAINWRIGHT. Sharp thresholds for high-dimensional and noisy sparsity recovery using ℓ_1-constrained quadratic programming (Lasso). *IEEE Trans. Information Theory*, 55:2183–2202, May 2009. MR2729873

[30] W. B. WU AND M. POURAHMADI. Nonparametric estimation of large covariance matrices of longitudinal data. *Biometrika*, 90(4):831–844, 2003. MR2024760

[31] M. YUAN AND Y. LIN. Model selection and estimation in the Gaussian graphical model. *Biometrika*, 94(1):19–35, 2007. MR2367824

[32] P. ZHAO AND B. YU. On model selection consistency of Lasso. *Journal of Machine Learning Research*, 7:2541–2567, 2006. MR2274449

[33] S. ZHOU, J. LAFFERTY, AND L. WASSERMAN. Time-varying undirected graphs. In *21st Annual Conference on Learning Theory (COLT)*, Helsinki, Finland, July 2008.